

2019

## Triggering depolymerization: Progress and opportunities for self-immolative polymers

Rebecca Yardley  
*Western University*

Amir Rabiee Kenaree  
*Western University*

Elizabeth Gillies  
*Western University, egillie@uwo.ca*

Follow this and additional works at: <https://ir.lib.uwo.ca/chempub>

 Part of the [Chemistry Commons](#)

---

### Citation of this paper:

Yardley, Rebecca; Rabiee Kenaree, Amir; and Gillies, Elizabeth, "Triggering depolymerization: Progress and opportunities for self-immolative polymers" (2019). *Chemistry Publications*. 127.  
<https://ir.lib.uwo.ca/chempub/127>

# Triggering depolymerization: Progress and opportunities for self-immolative polymers

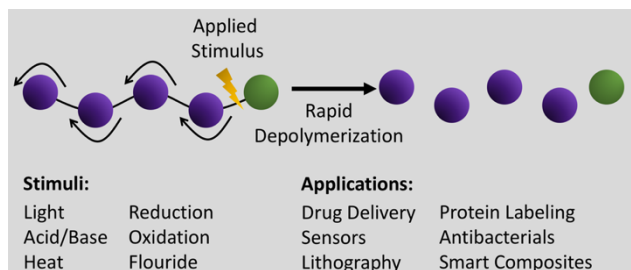
Rebecca E. Yardley,<sup>†</sup> Amir Rabiee Kenaree,<sup>†</sup> and Elizabeth R. Gillies\*<sup>†‡</sup>

<sup>†</sup> Department of Chemistry and the Centre for Advanced Materials and Biomaterials Research, The University of Western Ontario, 1151 Richmond St., London, Ontario, Canada N6A 5B7.

<sup>‡</sup> Department of Chemical and Biochemical Engineering, The University of Western Ontario, 1151 Richmond St., London, Ontario, Canada N6A 5B9.

\*Author to whom correspondence should be addressed: [egillie@uwo.ca](mailto:egillie@uwo.ca)

## Table of contents graphic



## Abstract

Polymers that depolymerize end-to-end upon cleavage of their backbones or end-caps, often referred to as “self-immolative” polymers (SIPs), have garnered significant interest in recent years.

They can be distinguished from other degradable and stimuli-responsive polymers by their ability to provide amplified responses to stimuli, as a single bond cleavage event is translated into the release of many small molecules through a cascade of reactions. Here, the synthesis and properties of the major classes of SIPs including poly(benzyl carbamate)s, poly(benzyl carbonate)s, polyphthalaldehydes, polyglyoxylates, polyglyoxylamides, poly(olefin sulfone)s, and poly(benzyl ether)s are presented. In addition, their advantages and limitations as well as their recent applications in areas including sensors, drug delivery, micro- and nano-patterning, transient devices and composites, coatings, antibacterial, and recyclable plastics are described. Finally, the challenges associated with the development of new SIP backbones and their translation into commercial products are discussed.

## **Introduction**

Many traditional applications of polymers have relied on their high long-term stability. For example, consumers rely on plastic beverage packaging to retain its structure and impermeability under a wide range of conditions and polyethylene used in joint replacements should resist degradation in the human body over a period of decades. In recent years however, there has been an increasing interest in polymers that can be readily degraded. This interest is on the one hand motivated by increasing attention to the global problem of plastic pollution.<sup>1-2</sup> At the same time, degradable polymers are of significant interest for the growing biomedical fields of drug delivery<sup>3</sup> and tissue engineering.<sup>4</sup> Much attention in the area of degradable polymers has focused on polysaccharides<sup>5</sup> and polyesters.<sup>6-7</sup> These polymers typically undergo a gradual degradation, either *in vivo* or in the environment. In many cases, a polymer would ideally remain highly stable while being used in its application, and then would degrade rapidly on demand under specified conditions.

While the concept of triggered depolymerization is not new, over the last decade there has been a resurgence of interest in depolymerization. In particular, significant progress has been made in our ability to trigger depolymerization with specific stimuli and in demonstrating its application in smart materials and devices. Inspired by the notion of self-destruction, polymers that depolymerize end-to-end upon triggering have often referred to as self-immolative polymers (SIPs).<sup>8</sup> Other naming conventions including continuous head-to-tail depolymerization<sup>9</sup> and cascade depolymerization<sup>10</sup> have also been used. We consider a defining feature of SIPs to be their ability to undergo complete end-to-end depolymerization following a single bond cleavage event by a stimulus. This provides an amplified response to the stimulus, as many molecules are released from a single stimulus event. End-to-end depolymerization can occur following the stimulus-mediated cleavage of a polymer end-cap (**Figure 1a**), or backbone bond of either a linear (**Figure 1b**) or cyclic SIP (**Figure 1c**).

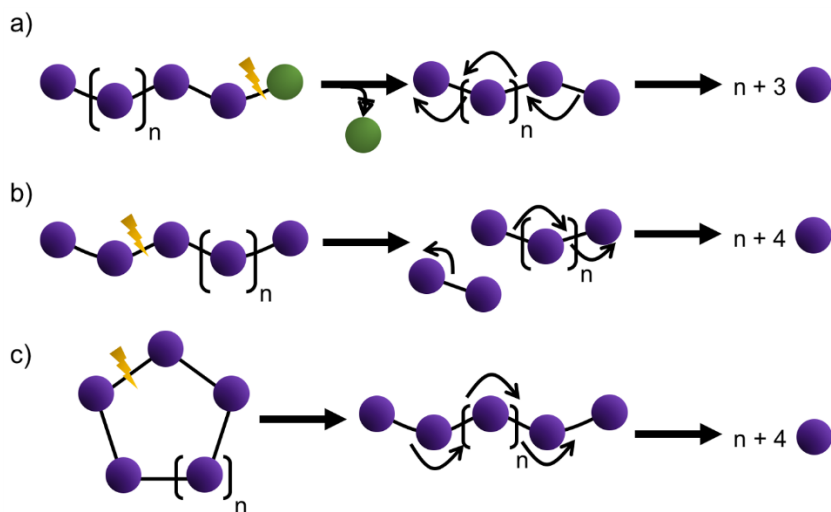


**Figure 1.** Depolymerization can be triggered by (a) end-cap cleavage; (b) backbone cleavage of a linear polymer; (c) backbone cleavage of a cyclic polymer. After the initial cleavage, the arrows represent a cascade of sequential reactions leading to depolymerization.

Depolymerizable SIP backbones can be categorized as either irreversible or reversible. Irreversible SIPs degrade to products that differ from the monomers from which they were synthesized, and therefore they cannot be repolymerized (**Figure 2a**). In contrast, reversible SIPs depolymerize to the monomers from which they were synthesized, making repolymerization possible, at least in principle (**Figure 2b**). The different SIP backbones and their derivatives vary widely in terms of their depolymerization rates, triggering chemistry, degradation products, as well as their thermal and mechanical properties. Therefore, they must be carefully selected and tuned according to the target application. Several comprehensive reviews on SIPs have been published over the years.<sup>9, 11-13</sup> In this perspective, we will focus on the current major classes of reversible and irreversible SIPs, highlighting the advantages and limitations of each based on literature reports as well as our perspective and practical experience. We will emphasize recent developments and application areas where SIPs can offer new functions beyond those of traditional degradable and stimuli-responsive polymers as well as the challenges that need to be addressed to go beyond the proof of concept studies.

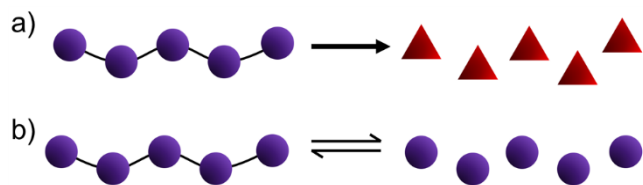


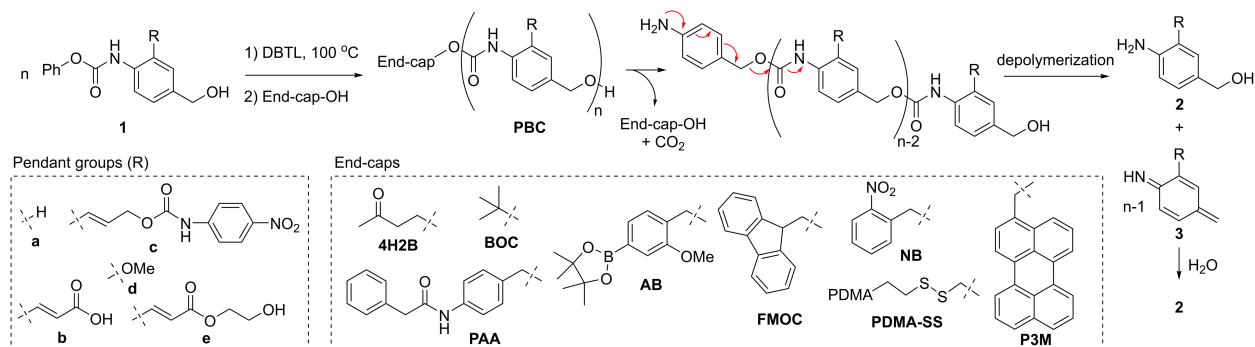
**Figure 2.** After end-cap or backbone cleavage, SIPs can **(a)** irreversibly depolymerize to molecules different from the original polymerization monomers or **(b)** reversibly depolymerize back to monomers.

## Irreversible SIPs

The first reported irreversible linear SIPs were inspired by self-immolative dendrimers.<sup>14-16</sup> Unlike the step-wise synthesis of dendrimers, the polymers were prepared in one-step reactions. Irreversible SIPs have been prepared by step-growth polymerizations and depolymerize by elimination and/or cyclization reactions. Poly(benzyl carbamate)s (PBCs) derived from 4-aminobenzyl alcohol have been the most widely used irreversible SIPs. Polycarbonates and variations incorporating different linkers have also been introduced to tune the depolymerization rate and to introduce new properties and functions. Proof of concept studies with these polymers in different applications such as sensors and drug delivery vehicles have been performed.

**Poly(benzyl carbamates) (PBCs).** The first PBC SIP was introduced by Shabat and coworkers in 2008.<sup>8</sup> A phenyl carbamate (**1**) was polymerized using dibutyltin dilaurate (DBTL) as a catalyst at 100 °C with an alcohol end-capping agent to afford **PBCa (Scheme 1)**. The polymerization reaction is quite versatile and a variety of functional monomers as well as different end-caps have been incorporated. PBCs have also been incorporated as depolymerizable side chains on bottlebrush polymers.<sup>17</sup> However, the degree of polymerization ( $DP_n$ ) has typically been limited to  $< 20$ , and the step-growth polymerization mechanism results in relatively broad dispersities ( $D$ ) ranging from  $\sim 1.4$ – $2.0$ . Following end-cap cleavage to reveal a terminal aniline, the depolymerization of PBCs is based on a 1,6-elimination-decarboxylation cascade.<sup>18</sup> The released azaquinone methides (**3**) react with water or other nucleophiles to generate 4-aminobenzyl alcohol or its derivatives (**2**). In the presence of water, the depolymerization is relatively rapid, reaching completion over several hours.<sup>8</sup> However, in less polar media the depolymerization reaction is very slow,<sup>19-21</sup> often requiring days. Phillips and coworkers accelerated the depolymerization rate of PBC oligomers through the introduction of electron-donating methoxy groups or by reduction

of the aromatic character of the repeat units using naphthalene derivatives.<sup>22</sup> Both of these approaches lowered the energetic costs of dearomatization involved in the depolymerization.



**Scheme 1.** Synthesis and depolymerization PBCs having different pendant groups and end-caps.

PBCs have been incorporated into a number of different sensor designs. Shabat and coworkers incorporated *ortho*-acrylate substituents onto a PBC and 4-hydroxy-2-butanone as an end-cap, resulting in the water soluble SIP **PBCb-4H2B**.<sup>8</sup> While the polymers were not fluorescent, cleavage of the end-cap by bovine serum albumin resulted in depolymerization to the corresponding aniline derivative, which fluoresced at 510 nm. Alternatively, 4-nitroaniline carbamates were incorporated as pendant groups, along with *ortho*-acrylates and a phenylacetamide end-cap (**Scheme 1, PBCb/c-PAA**).<sup>21</sup> Cleavage of the end-cap by penicillin-G amidase triggered backbone depolymerization by the 1,6-elimination-decarboxylation cascade and release of 4-nitroaniline reporters by an analogous pendant group fragmentation. Most recently, Shabat and coworkers also developed poly(benzyl carbonate)s that depolymerized to release quinone methides.<sup>23</sup> Schaap's adamantylidene-dioxetane turn-ON chemiluminescence probe was incorporated into each monomer unit such that trapping of the quinone methide by water generated a phenolate-dioxetane, which spontaneously decomposed by a chemically initiated electron-exchange process to generate an excited state benzoate and adamantanone. Emission of blue light

(499 nm) occurred as the benzoate decayed to the ground state. In all of the above examples, a key characteristic was the release of multiple reporter molecules in response to one end-cap cleavage, exemplifying the key amplification feature of SIPs. Signal amplification is particularly important for the fabrication of sensors as higher sensitivities provide better detection limits.<sup>24</sup>

Phillips and coworkers took a different approach for developing PBC-based sensors. Instead of employing released molecules to generate the signal, they exploited depolymerization as a solubility switch.<sup>25</sup> Paper-based devices were prepared using the polymer as a hydrophobic, water-impermeable layer. End-cap cleavage triggered depolymerization to water-soluble products, allowing water to wick through the layer and dissolve a dye to provide a colored visual read-out. H<sub>2</sub>O<sub>2</sub> was detected directly using an aryl boronate end-cap (**Scheme 1, PBCd-AB**), while Pb<sup>2+</sup> and Hg<sup>2+</sup> were detected using glucose oxidase (GOX) to generate H<sub>2</sub>O<sub>2</sub>, with the enzyme conjugated to an aptamer.<sup>25-26</sup> For example, in the case of Hg<sup>2+</sup>, binding of the metal to the aptamer resulted in the immobilization of GOX on the surfaces of beads, allowing it to locally generate H<sub>2</sub>O<sub>2</sub> in a defined location on the device. While the PBCs used in this work were technically oligomers (DP<sub>n</sub> = 2–8), they improved the device sensitivity by 10<sup>4</sup> compared to devices prepared using small molecules.

PBC-based materials have also been explored for encapsulation and release applications. The ability to achieve high degrees of payload release in response to subtle chemical stimuli can provide advantages over traditional stimuli-responsive polymers. For example, Moore and coworkers prepared microcapsules from PBCs (**Scheme 1, PBCe-BOC and PBCe-FMOC**).<sup>27</sup> The hydroxyl pendant groups of the PBCs were activated with 2,4-toluene diisocyanate, then microcapsules were prepared using an emulsion process with butandiol as a chain extender. The capsules prepared from BOC and FMOC end-capped polymers released their payload over 24 –

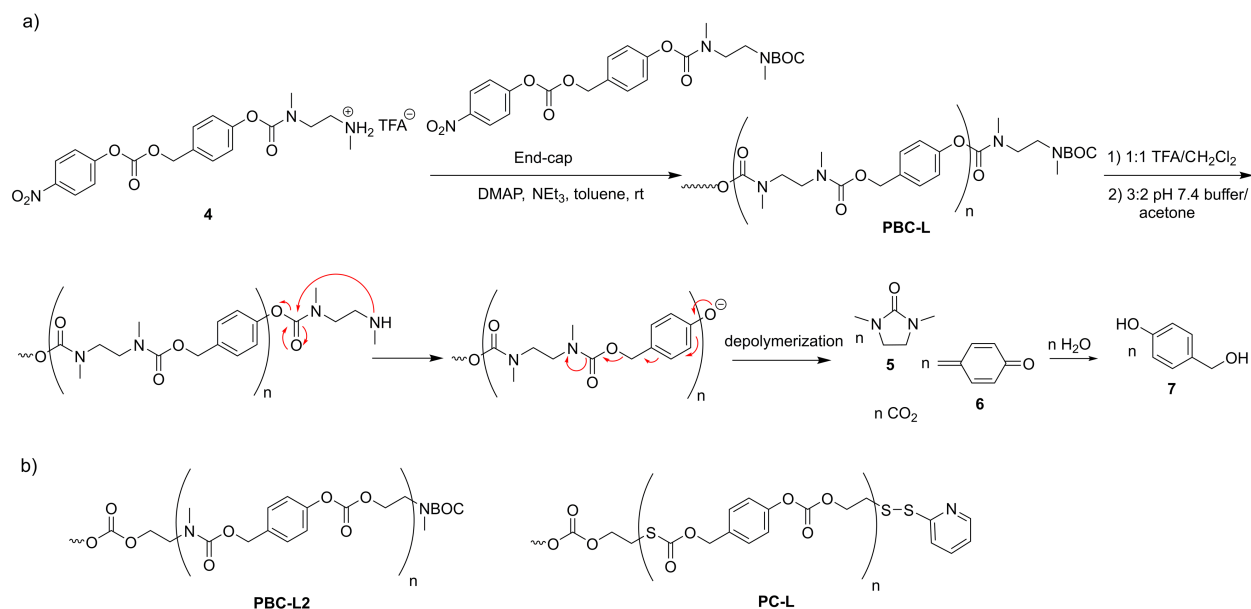


48 h using HCl and piperidine as stimuli respectively. Liu and coworkers also explored this concept by combining PBCs with hydrophilic poly(*N,N*-dimethylacrylamide) (PDMA) to afford amphiphilic block copolymers that self-assembled to form vesicles.<sup>28</sup> End-caps including perylene-3-ylmethyl carbamate (**P3M**), 2-nitrobenzyl carbamate (**NB**), and a PDMA-functionalized disulfide carbamate (**PDMA-SS**) were incorporated to enable triggering with visible light, UV light, and thiols respectively. Thiols in particular are biologically relevant stimuli as the reducing peptide glutathione is known to be present at higher concentrations in hypoxic tumors and also within cells compared to the extracellular environment.<sup>29</sup> Stimuli-triggered depolymerization of the SIP block and consequent vesicle disintegration resulted in the release of various payloads such as doxorubicin (DOX), camptothecin, and enzymes.

Shabat and coworkers also used PBCs for the activity-linked labeling of enzymes.<sup>30</sup> Penicillin-G amidase or the catalytic antibody Ab38C2 were used to trigger the end-cap cleavage of **PBCb-PAA** (**Scheme 1**). While the azaquinone methides released during depolymerization normally react rapidly with water molecules, their generation in the close vicinity of nucleophilic groups on the enzyme resulted in labeling of the proteins with the fluorescent 4-aminobenzyl alcohol derivatives. While promising for *in vitro* applications, the reactivity of azaquinone methides with proteins also provides a potential mechanism for toxicity which may hinder *in vivo* applications of PBCs.

**Polycarbamates containing linkers.** Cyclization spacers have been incorporated into SIPs to modulate their properties and depolymerization rates. In the early days of SIP development, our group began working on PBCs without pendant functional groups. They were poorly soluble in most solvents, which hindered our efforts to study their depolymerization. While Shabat and coworkers introduced pendant solubilizing groups, based on the known favorable cyclization of

*N,N'*-dimethylethylenediamine (DMED) derivatives to *N,N'*-dimethylimidazolidinones,<sup>31</sup> we inserted DMED spacers to improve the solubility.<sup>10</sup> The target SIP was synthesized from monomer **4**, containing a protonated amine (**Scheme 2a**). The addition of 4-dimethylaminopyridine (DMAP), NEt<sub>3</sub>, and BOC-protected monomer as an end-cap, afforded the BOC end-capped polycarbamate **PBC-L** with a DP<sub>n</sub> of ~16 and *D* of 1.6. Depolymerization was triggered by cleavage of the BOC group with trifluoroacetic acid (TFA) then immersion in pH 7.4 phosphate buffer:acetone (3:2). It occurred by a cascade of cyclization-1,6-elimination-decarboxylation reactions, requiring about 3 days to reach completion.



**Scheme 2.** (a) Synthesis and depolymerization of a polycarbamate based on 4-hydroxybenzyl alcohol and DMED (**PBC-L**); (b) Chemical structures of related analogues containing 2-methylaminoethanol (**PBC-L2**) or mercaptoethanol (**PC-L**) spacers.

We also incorporated different cyclization spacers (**Scheme 2b**).<sup>32</sup> For example, the replacement of DMED with 2-methylaminoethanol in **PBC-L2** or the mercaptoethanol spacer in **PC-L** resulted in more rapid cyclization reactions. While **PBC-L** required 7 h to reach 50%

depolymerization after triggering, **PBC-L2** was 50% degraded in 1 h, and polymer **PC-L** was 50% degraded in less than 30 min. Thus, the insertion of cyclization spacers allowed tuning of the depolymerization rate. However, a limitation of all of these backbones is the tendency to form cyclic oligomers during the polymerization (~20 wt%). These cyclic species are difficult to separate from the desired linear polymers and do not depolymerize upon end-cap cleavage as they do not possess end-caps. Cyclic species have not been reported for PBCs (**Scheme 1**), likely because their more rigid structures make intramolecular cyclization less favorable.

Polycarbamates with linkers were the first SIPs incorporated into block copolymers and used in encapsulation and release studies.<sup>10</sup> For example, we prepared an amphiphilic block copolymer by conjugating a hydrophilic PEG block to the end-cap of the hydrophobic SIP block. The resulting block copolymer **PBC-PEG (Figure 3a)** was self-assembled to form nanoparticles. Hydrolysis of the ester linkage between PEG and the SIP block resulted in the depolymerization of the SIP and degradation of the nanoparticles. Nile red, a hydrophobic dye molecule, was encapsulated into the SIP nanoparticles and was released as the nanoparticles degraded. In recent work, we used thermo-responsive poly(2-(dimethylamino)ethyl methacrylate) (PDMAEMA) as a hydrophilic block conjugated by a UV light-responsive linker end-cap (**Figure 3b, PBC-PDMAEMA**). **PBC-PDMAEMA** was self-assembled to form nanoparticles and we hypothesized that chain collapse of the PDMAEMA at elevated temperatures might increase the hydrophobicity of the SIP environment, slowing its depolymerization. However, the faster rate of background reactions at the temperatures required for the chain collapse of the PDMAEMA (60 °C) made it impossible to observe the anticipated effects of PDMAEMA chain collapse. In the future, it may be ideal to use a polymer such as poly(*N*-isopropylacrylamide), which has a lower cloud point temperature.<sup>33</sup>

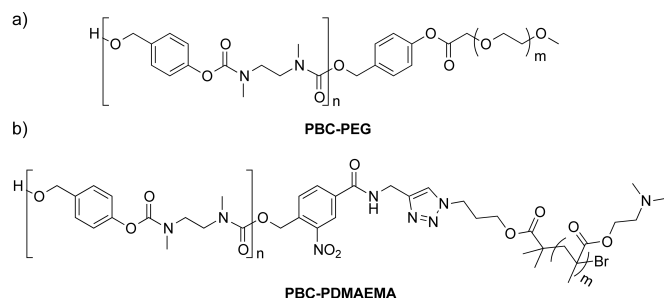
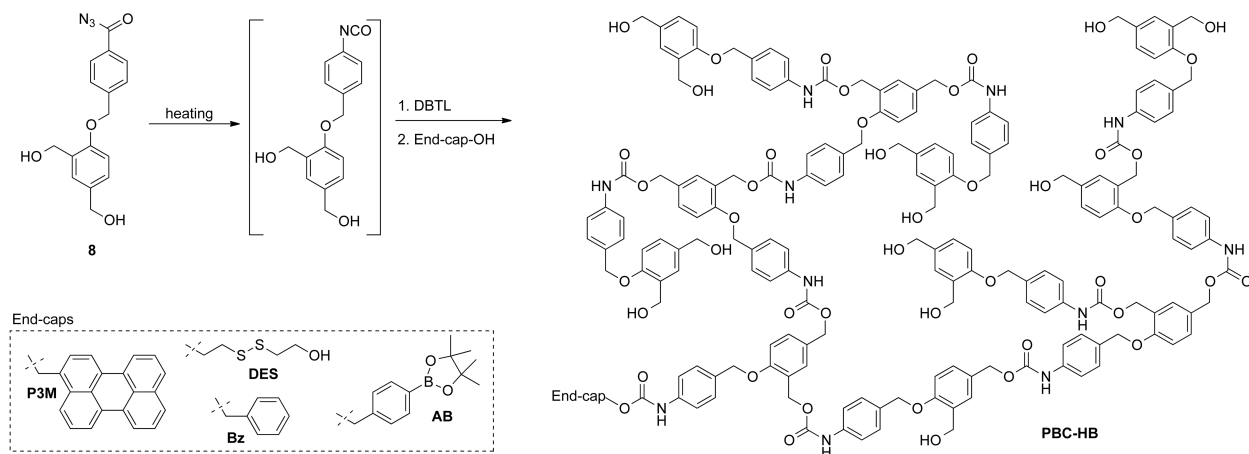


**Figure 3.** Structures of PBC-L block copolymers with (a) PEG and (b) PDMAEMA.

Almutairi and coworkers incorporated end-caps responsive to UV and near-infrared (NIR) light onto **PBC-L** and prepared nanoparticles from the resulting polymers using an emulsion process.<sup>34</sup> The nanoparticles were degraded using UV or NIR light and released Nile red in response to these stimuli. The cytotoxicity of the polymers and their degradation products were also explored. The materials were found to be as well tolerated as poly(lactic-*co*-glycolic) acid, which is approved in certain clinical applications. Nevertheless, like the poly(benzyl carbamate)s described above, this class of polycarbamates releases azaquinone methides during their depolymerization and further investigations of potential toxicity are required.

**Hyperbranched polycarbamates containing linkers.** Liu and coworkers inserted benzyl ether linkers into poly(benzyl carbamate)s to synthesize hyperbranched SIPs.<sup>35</sup> The linkers were necessary to prevent intramolecular cyclization. The incorporation of self-immolative benzyl ether linkages enabled the polymerization of monomers such as **8** to afford hyperbranched polymers using DBTL as a catalyst at 110 °C (e.g., **Scheme 3**, **PBC-HB**). Different end-caps were incorporated, such as **P3M**, **AB**, and diethanol disulfide (**DES**), and different backbone variations including benzyl thioethers were also synthesized, leading to polymers with  $M_n$  values of ~6–7 kg/mol and  $D$  of 1.5–1.7. PEG and PDMAEMA were appended to the terminal hydroxyls, leading to amphiphilic copolymers. The PEG copolymers were dispersed in water and loaded with small

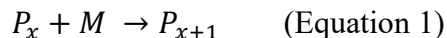
molecules such as DOX. Treatment with the stimulus, such as blue light for the **P3M** end-cap, led to release of the DOX over a few hours, even within cells. The cationic PDMAEMA chains were used to complex DNA and it was released upon treatment with glutathione for the **DES** end-capped system. Mitochondrial targeting through functionalization of the peripheral hydroxyls with CGKRK peptides was also explored, and the depolymerization of the **AB** capped polymer by endogenous  $H_2O_2$  was demonstrated through the release of a fluorescent reporter. Colorimetric detection of  $H_2O_2$  was achieved using gold nanoparticles combined with an enzymatic amplification sequence. In their *in vitro* studies, the authors did observe some cytotoxicity from the depolymerization products, suggesting that chemical and enzymatic assays may be more promising than *in vivo* applications.



**Scheme 3.** Synthesis of a hyperbranched polycarbamate.

## Reversible SIPs

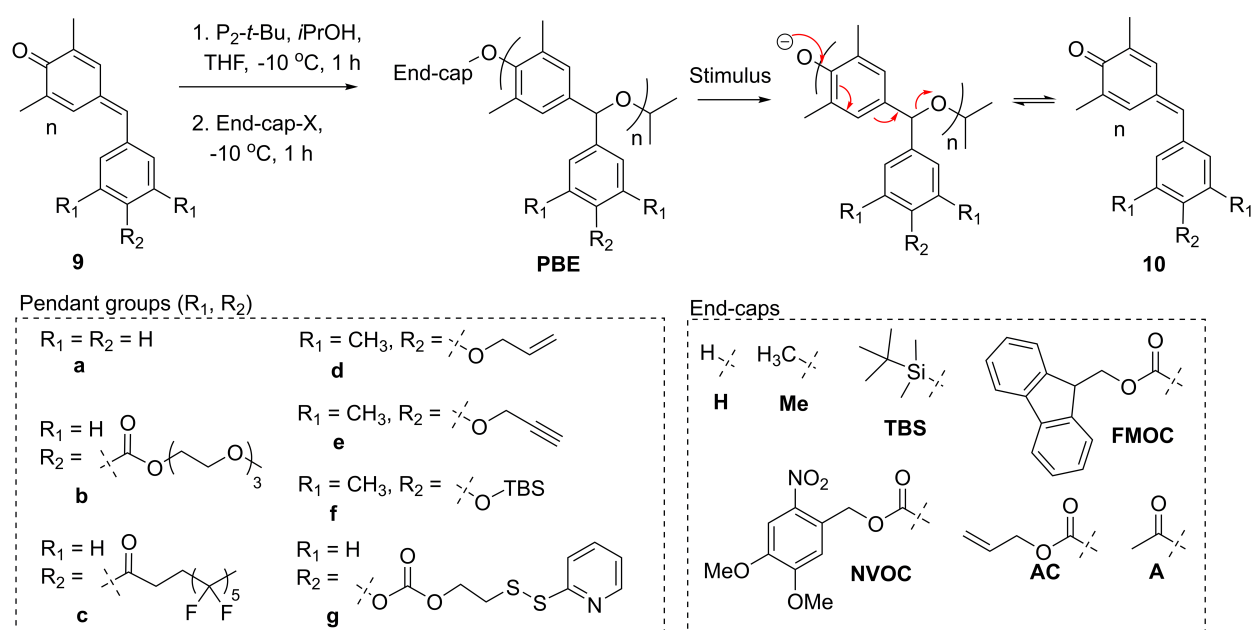
Reversible SIPs are typically based on polymers with low (i.e., below room temperature) ceiling temperatures ( $T_c$ ), where  $T_c$  is defined as the temperature above which, polymer of high molar mass is not formed in a given chain polymerization:<sup>36</sup>



where  $P_x$  is the growing chain with DP of  $x$  and  $M$  is a monomer. By definition, at the ceiling temperature  $\Delta G = 0$  for Equation 1, and consequently  $T_c = \Delta H/\Delta S$ . Thus, the ceiling temperature for a given polymerization depends on both enthalpic and entropic contributions.  $T_c$  also depends on the initial monomer concentration, and  $T_c(c^0)$  denotes the ceiling temperature for an initial monomer concentration of 1 M, while  $T_c(\text{bulk})$  denotes the ceiling temperature for undiluted monomer. Polymers can be synthesized below the  $T_c$ , but above the  $T_c$ , depolymerization occurs spontaneously. Capping or cyclization of the polymer below its  $T_c$  prevents the depolymerization, but when the end-cap or backbone is cleaved at room temperature, depolymerization can occur. Many of the reversible SIP backbones have actually been known for decades, but in the past decade, there have been significant developments in the introduction of stimuli-responsive end-caps that enable depolymerization to be triggered by a wide range of stimuli. This has facilitated the application of triggered depolymerization in diverse fields ranging from smart composites to drug delivery. Their depolymerization back to the monomers from which they were initially synthesized also endows reversible SIPs with the potential to be recycled through depolymerization and subsequent repolymerization. The most important classes of reversible SIPs are poly(benzyl ether)s, polyphthalaldehydes, polyglyoxylates, polyglyoxylamides, and poly(olefin sulfone)s.

**Poly(benzyl ether)s (PBEs).** Inspired by the work of McGrath and coworkers on PBE dendrimers,<sup>16</sup> as well as prior work on the anionic polymerization of quinone methides,<sup>37</sup> Phillips and coworkers introduced depolymerizable PBEs.<sup>38</sup> They polymerized 2,6-dimethyl-7-phenyl-1,4-benzoquinone **(9a)** using 1-*tert*-butyl-2,2,4,4,4-pentakis(dimethylamino)-2 $\lambda^5$ ,4 $\lambda^5$ -catenadi(phosphazene) ( $P_2$ -*t*-Bu) and an alcohol initiator at low temperatures (-10 to -20 °C) to

afford polymer **PBEa** with high  $DP_{nS}$ , up to 2300 and  $D$  of 1.3–1.5 (**Scheme 4**). The methyl groups on monomer **9a** were incorporated to prevent the uncontrolled polymerization<sup>37</sup> and the phenyl moiety was incorporated to make depolymerization more favorable, as extended conjugation stabilizes the initial quinone methide depolymerization product compared to the (aza)quinone methides generated in the depolymerization of the polycarbamates and polycarbonates described above. End-capping was performed using chloroformates or alkyl or silyl chlorides to afford the corresponding PBEs responsive to light, fluoride, acidic environments and redox reactions.



**Scheme 4.** Synthesis and depolymerization of PBEs with different pendant groups and end-caps.

The ether backbone imparted higher stability to PBEs compared with other backbones such as PBCs when exposed to base, acid, and heat. However, they depolymerized by 1,6-elimination reactions (**Scheme 4**) in less than 1 h when exposed to stimuli, even in organic solvents. Different groups such as tri(ethylene glycol)s,<sup>39</sup> fluoroalkyl chains,<sup>39</sup> alkenes for thiol-ene reactions,<sup>40-41</sup> alkynes for CuAAC,<sup>42</sup> and masked self-immolative moieties,<sup>43</sup> were incorporated onto the pendant phenyl ring of PBEs (**Scheme 4, PBEb-f**). Furthermore, Zhang and coworkers prepared

bottlebrush PBEs by grafting PEG or polystyrene (PS) side chains.<sup>42</sup> Interestingly, the PS-grafted polymer depolymerized more slowly, which was attributed to conformational constraints that made it more difficult for the backbone to attain the ideal geometry for the 1,6-elimination reaction.

Phillips and coworkers explored the triggered depolymerization of PBEs in the solid state. They combined hydrogen-terminated PBEs (**PBEb-H** and **PBEc-H**) with other polymers such as PS, polyethylene, and polypropylene, resulting in mixtures of plastics that could not be separated based on properties such as solubility.<sup>39</sup> Addition of the base 1,8-diazabicyclo[5.4.0]undec-7-ene (DBU) resulted in selective depolymerization of the PBE in about 2 h at 23 °C (**Figure 4**). After recovering the monomers by extraction, they were repolymerized to afford PBE in 83% yield, compared to 87% yield for the original polymerization. Optimization of aspects such as cost and efficiency of monomer recovery would be required, but this was an interesting proof of concept for the use of SIPs in mixed plastic recycling.

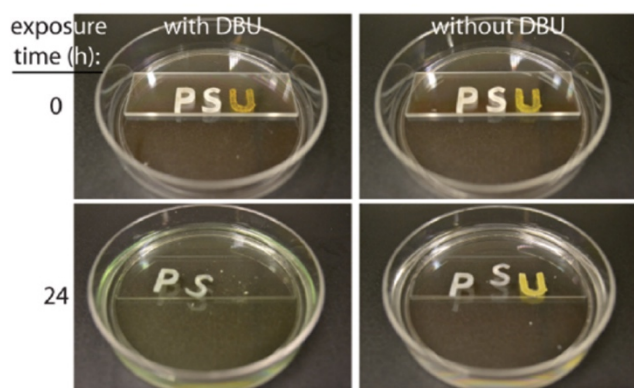


**Figure 4.** Separation of solid PBE (U) from solid polyethylene (P) and polypropylene (S) by selective depolymerization induced by DBU. Adapted with permission from reference <sup>39</sup>. Copyright 2015, Royal Society of Chemistry.



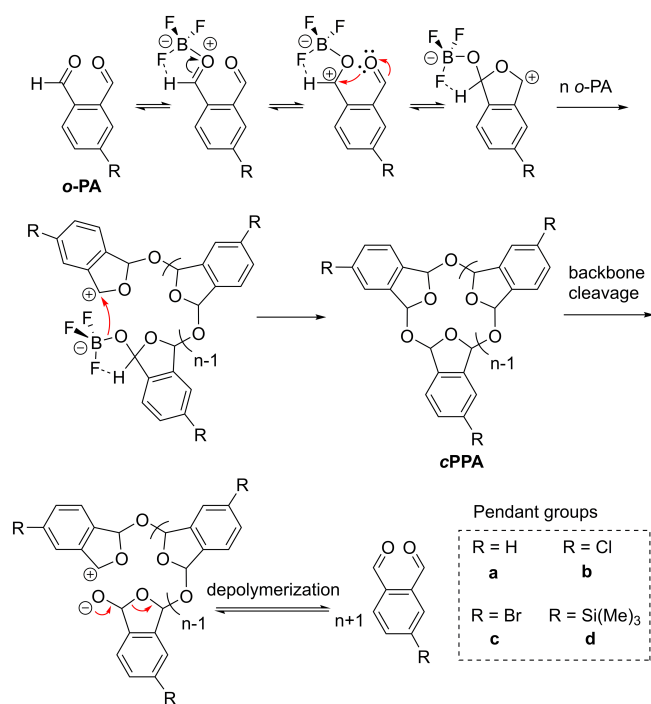
While depolymerization occurred for the hydrogen-capped PBE in 2 h with DBU,<sup>39</sup> Phillips and coworkers also noted that the depolymerization of most PBEs was very slow in the solid state.<sup>43</sup> They attributed this to a lack of accessible end-caps at the solid-liquid interface, and therefore incorporated stimuli-responsive triggers, such as TBS-protected phenols, on each backbone repeat unit (e.g., **PBEf-A**, **Scheme 4**). Cleavage of these moieties resulted in 1,6-elimination reactions of the resulting phenols, cleaving the backbone. Rigid polymer disks prepared from polymer **PBEf-A** were depolymerized to soluble products in less than 5 h in the presence of fluoride ions at 23 °C. In a related approach, Zhang and coworkers reported PBEs with pendant disulfide groups (**PBEg-TBS**, **Scheme 4**).<sup>44</sup> Conjugation of PEG-SH *via* disulfide exchange led to graft copolymers, while reaction with HS-PEG-SH led to gels. The materials were degraded by a reducing agent (DTT), as the released thiol cyclized onto the carbonate group, releasing the phenol, which underwent a 1,6-elimination to initiate the depolymerization. In these latter two examples, the cleavage of the PBE through the pendant groups resulted in one fragment terminated with a phenol, that depolymerized, and another fragment terminated with a benzylic alcohol, which did not immediately depolymerize. In this sense, PBEs differ from polyaldehydes where backbone cleavage results in two unstable fragments as described in the next sections.

Ergene and Palermo explored cationic PBEs as potential antibacterial polymers.<sup>40-41</sup> They grafted primary and tertiary amines as well as quaternary ammonium groups onto alkene-functionalized PBEs using thiol-ene chemistry (**PBEd-TBS**, **Scheme 4**). The primary amine-functionalized PBEs had the highest activities. The tertiary amine-functionalized PBEs were much less active, and the quaternary ammonium systems had intermediate activities. Hemolysis, the lysis of red blood cells, often serves as an initial indicator of toxicity to mammalian cells. The primary and tertiary amine-functionalized PBEs were highly hemolytic, but the quaternary ammonium-

functionalized PBE was much less hemolytic. Depolymerization of the primary ammonium-functionalized polymer, induced by fluoride, greatly reduced its hemolytic toxicity, while retaining high antibacterial activity. In follow-up work, Ergene and Palermo grafted varying ratios of PEG and primary amines to **PBEd-TBS** to modulate their hydrophobic-hydrophilic balance.<sup>45</sup> With 25–50 mol% of 800 g/mol PEG, high antibacterial activities were retained while reducing hemolytic activities, and only minor changes in these activities were observed upon depolymerization. In contrast, grafting of 2000 g/mol PEG resulted in similar decreases in antibacterial and hemolytic activities. Overall, this work demonstrates a potential role for depolymerization in modulating the behavior of antibacterial polymers. Further work will be needed to determine the toxicity of the PBEs and their depolymerization products. The authors also noted the potential for SIPs in the development of antibiofilm coatings with a triggerable self-cleaning characteristic. Some initial efforts towards this approach were recently reported by Lienkamp and coworkers in collaboration with our group using UV light-sensitive PEtG as a sheddable coating layer.<sup>46</sup>

**Polyphthalaldehydes (PPAs).** PPAs are polyacetals composed of *o*-phthalaldehyde (*o*-PA) or its derivatives.<sup>47</sup> Because of the relatively small enthalpy change associated with the conversion of the aldehyde's carbon-oxygen double bond to two carbon-oxygen single bonds in the polymer, the entropy gained through depolymerization overrides the enthalpic cost of depolymerization at relatively low temperatures, leading to low  $T_c$  values (e.g., -40 °C for *o*-PPA).<sup>48</sup> Metastable PPAs can be prepared *via* cyclization or end-capping reactions, but when terminal hemiacetal moieties are revealed through either a backbone or end-cap cleavage, they rapidly depolymerize to the monomers at ambient temperatures. Significant advancements have been made in both the synthesis and application of PPAs over the past decade.

**Cyclic polyphthalaldehydes.** In 1960s, Aso and Tagami studied different acid catalysts for the polymerization of *o*-PA, including  $\text{BF}_3 \cdot \text{OEt}_2$  (**Scheme 5**),  $\text{TiCl}_4$ ,  $\text{SnCl}_4$ , and  $[\text{Ph}_3\text{C}][\text{BF}_4]$  at  $-78^\circ\text{C}$  and suggested cyclic structures of the polymers (**cPPAa**).<sup>49-50</sup> The polymerizations were rapid (less than 1 h) but they could not control the  $\text{DP}_n$  of the isolated PPAs. Ito and coworkers used  $\text{BF}_3 \cdot \text{OEt}_2$  for the polymerization of *o*-PA derivatives including 4-chlorophthalaldehyde, 4-bromophthalaldehyde, and 4-trimethylsilylphthalaldehyde affording **cPPAb-d**.<sup>51</sup> The electron-withdrawing groups made the backbones less susceptible to cleavage. Moore and coworkers finally confirmed the cyclic structures of cationically synthesized PPAs *via* end-group analysis using NMR spectroscopy and mass spectrometry.<sup>52</sup> They also discovered that under cationic conditions, the cyclic polyacetal backbone of PPAs could reversibly cleave to release or incorporate monomers before backbiting and forming the final cyclic polymers. Taking advantage of this scrambling mechanism, they prepared random and multi-block copolymers by simply mixing PPAs with different derivatives of *o*-PA (**Figure 5**).<sup>53</sup> Kohl and coworkers later suggested that the  $\text{BF}_3 \cdot \text{OEt}_2$  mediated synthesis of PPAs involves zwitterionic intermediates and that the interactions of two chain ends with opposite charges allows the ring formation events.<sup>54</sup>



**Scheme 5.**  $\text{BF}_3 \cdot \text{OEt}_2$  catalyzed polymerization of *o*-PA and its derivatives to give PPAs. Cleavage of the backbone leads to depolymerization to the corresponding monomers.

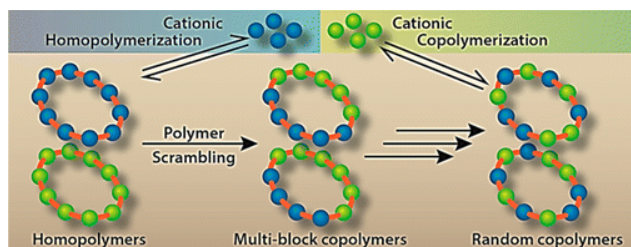


**Figure 5.** Block and random cyclic copolymers of *o*-PA can be prepared by a reversible opening and closing of the cyclic PPA backbone. Adapted with permission from reference <sup>53</sup>. Copyright 2013, American Chemical Society.

Kohl and coworkers also recently employed  $\text{BF}_3 \cdot \text{OEt}_2$  to copolymerize *o*-PA with a series of aliphatic aldehydes.<sup>55</sup> The copolymerization yield and average molar mass decreased by increasing the aliphatic aldehyde feed percentage. However, the mechanical properties of the lower

molar mass copolymers were enhanced by cross-linking using radiation-induced thiol–ene click chemistry. These results were important as pure PPAs are highly brittle, and the copolymerization strategy provided access to a range of PPA-based copolymers with varying mechanical properties and also functional groups. As for many commercial plastics, the properties of PPA have also been tuned through the incorporation of additives. For example, Sottos and coworkers showed that remaining solvents, such as  $\text{CHCl}_3$ ,  $\text{CH}_2\text{Cl}_2$ , or dioxane, from a solvent-casting process could serve as plasticizers and change the mechanical properties of PPA films.<sup>56</sup> For example, depending on the solvent, they found different elastic moduli (2.5–3 GPa), tensile strengths (25–35 MPa), failure strains (1–1.5%), and  $T_g$  values (64–95 °C). The additive strategy was also explored by Kohl and coworkers through the incorporation of ionic-liquid and ether-ester plasticizers.<sup>57</sup> Their study showed that plasticizers changed the thermal stability and mechanical properties. For example, 20 parts per hundred bis(2-ethylhexyl) phthalate (BEHP) reduced the storage modulus to *ca.* 1.2 MPa, which is about half that of pure *o*-PPA. In addition, the additives lowered the melting point of the degradation products from 54.3 °C (pure *o*-PA) to 37.5 °C (for formulated mixtures), which enabled the degradation products to better maintain the liquid state. This can potentially improve the transient nature of PPA devices by allowing them to be more readily absorbed into the environment.

Cyclic PPAs are metastable solids due to their susceptibility to backbone cleavage and depolymerization. This feature has garnered interest for a number of applications. Early work focused on lithography applications, wherein a resist was patterned using a depolymerization-inducing beam to dry-develop a pattern. Ito and Willson initially exploited the pH-sensitivity of PPA's acetal backbone by combining the polymer with photoacid generators (PAGs).<sup>58</sup> In their early studies using linear PPAs, good light sensitivity and pattern development were observed.<sup>59-</sup>

<sup>60</sup> However, the required formulations were too sensitive and the depolymerization product *o*-PA contaminated the expensive optics. They also investigated the more stable halogenated derivatives **cPPAb** and **cPPAc**.<sup>51</sup> However, they were not able to self-develop at temperatures below 100 °C and required a postbaking step.

More recently, the groups of White, Rogers, and Moore fabricated transient electronics based on cyclic PPAs.<sup>61</sup> They combined PPA with a PAG to create substrates for free-standing transistor arrays. Upon exposure to a UV light (379 nm), acid-triggered depolymerization led to disintegration of the array (**Figure 6a**). They also prepared thermally-triggerable transient electronics based on PPAs layered with an acid microdroplet-containing wax.<sup>62</sup> Melting the wax released the acid, resulting in rapid device destruction (**Figure 6b**). Kohl and coworkers also explored strategies for the fabrication of PPA-based electronics.<sup>63</sup> For example, they prepared materials by layering PAG-free PPA with a thin layer of PPA/PAG blend and showed that this method improved the shelf life of the materials.<sup>64</sup> Building on this work, they investigated the application of different polynuclear aromatic hydrocarbons as PAGs and showed that the combination of a pentacene-based sensitizer with PPAs afforded a transient material able to depolymerize after 1 min in direct sunlight.<sup>65</sup>

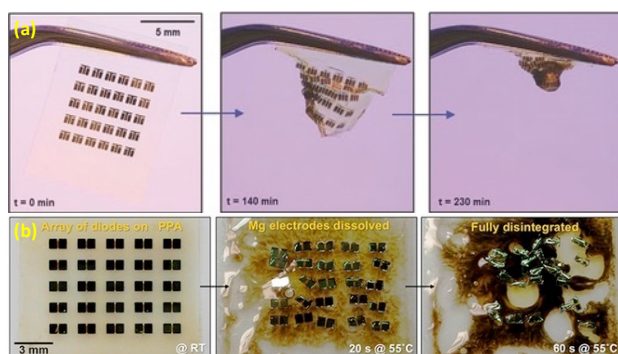


**Figure 6.** Acid release and destruction of PPA-based transistor arrays due to **(a)** the activity of a photoacid generator after irradiation with UV light and **(b)** melting an acid microdroplet-

containing wax within the PPA. Adapted with permission from reference <sup>61</sup> (a) and reference <sup>62</sup> (b). Copyright 2014, John Wiley and Sons.

Mechanically-triggered depolymerization of cyclic PPA has also been investigated by Moore, Boydston, and coworkers.<sup>66</sup> Their study showed that for PPA above a critical molar mass of about 30 kg/mol, mechanical forces applied using pulsed ultrasound induced heterolytic chain scission, created hemiacetalate and oxocarbenium chain ends, leading to subsequent depolymerization. Exploiting the potentially reversible depolymerization back to monomer, they recycled 67% of the resulting *o*-PA and repolymerized it to produce high molar mass PPA.

Moore and coworkers used cyclic PPAs for ion-triggered release of payloads from microcapsules.<sup>67</sup> The core-shell microcapsules were prepared by emulsification followed by rapid solvent evaporation, and were then suspended in acidic solutions with or without coactivating salts such as LiCl. The microcapsules selectively depolymerized in the presence of specific ions and released their contents due to a specific ion coactivation effect. White, Moore, Sottos, and coworkers also recently reported *o*-PPA-based composites which can be quantitatively recycled.<sup>68</sup> As PPAs are not thermally stable, a 14 min heat treatment at 120 °C was sufficient to fully disintegrate the composite and yield the monomer in addition to the reinforcing materials before reusing them to reproduce the identical composites (**Figure 7**). Even after three full cycles of depolymerization and repolymerization, the composites retained the same moduli (4.5 GPa) and tensile strengths (30 MPa).

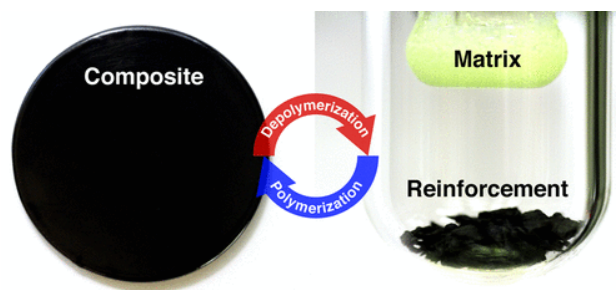
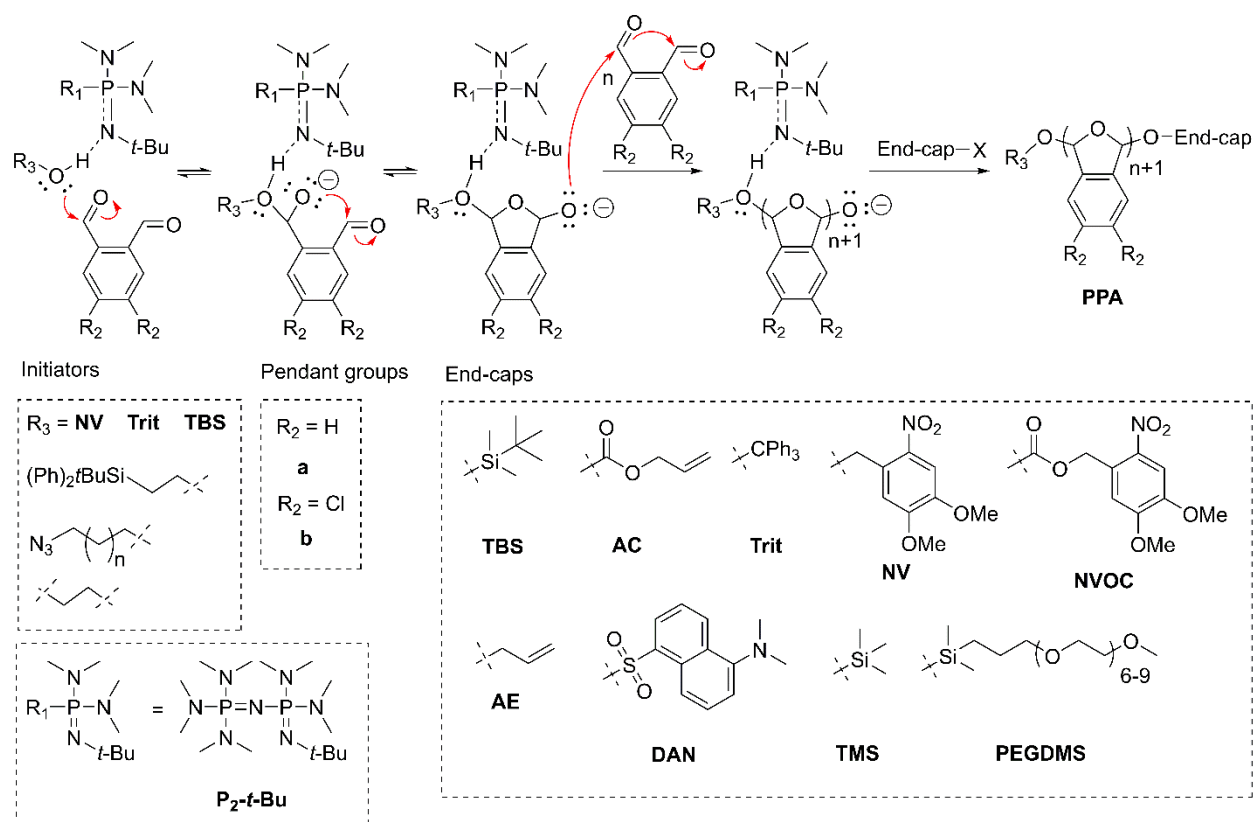


**Figure 7.** Composites composed of carbon fiber and PPA (left) can be fully disintegrated to the starting carbon fiber (right, bottom) and *o*-PA (right, top) before the reproduction of the composite. Adapted with permission from reference <sup>68</sup>. Copyright 2019, American Chemical Society.

**Linear polyphthalaldehydes.** Linear PPAs can be produced by anionic polymerization methods as the propagating species have only one charged terminus and thus the chance of cyclization by backbiting onto the other neutral terminus is negligible. In early work, Aso and Tagami used anionic initiators including *t*-BuOLi, Na with naphthalene, and Na with benzophenone to prepare linear PPAs.<sup>69</sup> End-capping was performed with reagents such as acetic anhydride. Similar to *c*PPA, the backbones of linear PPAs can be cleaved using heat, acid, or mechanical force. To enable PPA cleavage using different stimuli, Phillips and coworkers incorporated different end-caps. Using an *n*-BuLi-initiated *o*-PA polymerization, they introduced fluoride ion-responsive *t*-butyldimethylsilyl (TBS) and Pd(0)-responsive allyl carbonate (AC) end-caps.<sup>70</sup> However, the polymerization reactions were slow (3–12 days) and showed a negative deviation from the targeted DP<sub>n</sub> values. Building on a work by Hedrick, Knoll, and Coulembier, showing that phosphazene superbases served as suitable initiators for rapid and well-controlled polymerization of *o*-PA,<sup>71-72</sup> Phillips and coworkers used P<sub>2</sub>-*t*-Bu with functional alcohol initiators to successfully polymerize *o*-PA in 3 h, and directly installed stimuli-responsive end-caps (**Scheme 6**).<sup>73-74</sup> Depolymerization was successfully triggered using stimuli corresponding to the specific end-caps.





**Scheme 6.** Anionic polymerization of PAs using phosphazene and various responsive end-caps.

As the synthesis of different *o*-PA derivatives is tedious, a limited number of linear PPA derivatives have been reported. Phillips and coworkers used the phosphazene/alcohol initiated polymerization method to prepare poly(4,5-dichlorophthalaldehyde)s (**PPAb**, Scheme 6).<sup>75</sup> Post-polymerization modification is an alternative approach to modify the structure and properties of PPAs. Moore and coworkers used the phosphazene/alcohol initiated polymerization to copolymerize benzaldehyde derivatives with *o*-PA, resulting in random copolymers with functional groups for post-polymerization reactions.<sup>76-77</sup> Pendant nitrophenyl, bromophenyl, aldehyde, alkene, alkyne, imine, and hydroxyl groups were then used for the formation of nanoparticles, networks, and graft copolymers.

As noted above, linear PPAs were investigated in early lithography applications with PAGs due to the intrinsic acid-sensitivity of their polyacetal backbones.<sup>59-60</sup> More recently, Knoll, Duerig, and coworkers exploited their intrinsic thermo-sensitivity in thermal scanning probe nanolithography (t-SPL).<sup>78-79</sup> In this method, a cantilever, resting at *ca.* 300 nm above the surface, was heated to 700 °C and created a 3-D pattern by the thermal depolymerization of a PPA film. The pattern could also be transferred to the silicon substrate by reactive ion etching (RIE) (**Figure 8**).<sup>71, 80</sup> Taking advantage of the high precision of t-SPL, a PPA pattern was created for a sorting device that separated 60- and 100-nm particles in opposing directions in seconds.<sup>81</sup>

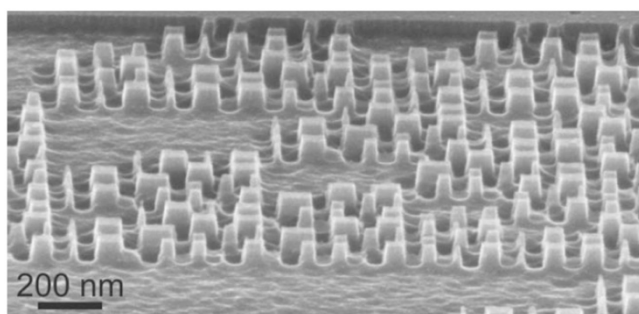


**Figure 8.** Scanning electron micrograph of a nanoscale pattern prepared by t-SPL of a PPA film followed by transfer to a silicon substrate by RIE. Adapted with permission from reference <sup>80</sup>. Copyright 2010, John Wiley and Sons.

Phillips and coworkers have employed PPA end-cap cleavage in their applications. In their early work, they prepared stimuli-responsive plastics *via* patterning of a TBS end-capped PPA within a control allyl ether (AE)-capped PPA (**PPAa-TBS** and **PPAa-AE**, **Scheme 6**).<sup>70</sup> The depolymerization of **PPAa-TBS** was induced with fluoride ion, and resulted in a cylindrical hole. Using **PPAa-TBS**, they also prepared microcapsules with aqueous cores containing fluorescein-labeled dextran.<sup>74</sup> Exposure to fluoride ion resulted in holes in the capsule wall, causing release of the dextran. Exploiting its high stability, Phillips and coworkers later created multi-layered macroscopic patterns composed of **PPAb** with different stimuli-responsive end-caps.<sup>75</sup> Different

layers were selectively degraded in the presence of specific stimuli such as Pd(0) and fluoride ion (Figure 9). They have also fabricated self-powered microscale pumps which generated flow based on the depolymerization of PPAa-TBS to soluble monomers in the presence of fluoride ions.<sup>82</sup>

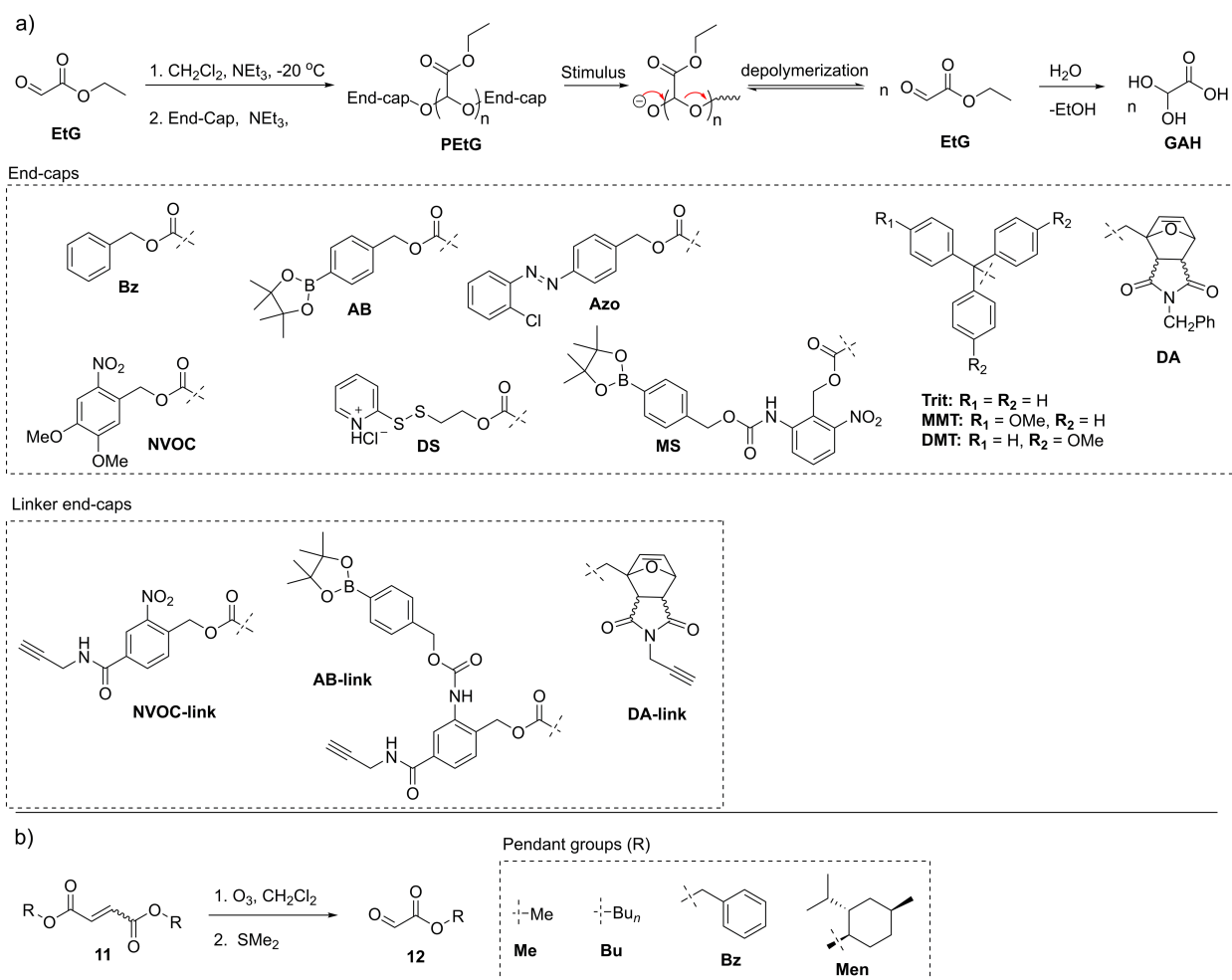


**Figure 9.** Visual ion sensors based on PPAb (red triangles, blue circles, and yellow grids are Pd(0), fluoride ion, and non-responsive PPAs respectively). Adapted with permission from reference <sup>75</sup>. Copyright 2015, John Wiley and Sons.

**Polyglyoxylates (PGs).** PGs are another class of polyaldehydes that exhibit low  $T_c$ , and consequently undergo depolymerization following an end-cap or backbone cleavage. Poly(ethyl glyoxylate) (PEtG),<sup>83</sup> poly(methyl glyoxylate) (PMeG),<sup>84</sup> and poly(glyoxylic acid) salts<sup>85</sup> were reported over the past few decades and were initially stabilized through end-capping with isocyanates or vinyl ethers. With these end-caps, PGs degraded gradually by the hydrolysis of the pendant esters, backbone acetal cleavage, and backbone depolymerization, leading to the corresponding alcohols and glyoxylic acid hydrate (GAH).<sup>86</sup> The conversion of GAH to CO<sub>2</sub> occurs through the glyoxylic acid cycle, an anaerobic variant of the Krebs's cycle, which occurs in bacteria, plants, and protists. The degradation products of PEtG were found to be non-toxic to plants and also in an invertebrate model.<sup>87</sup> GAH is also a metabolic intermediate that can be processed in the human liver, so it is anticipated to be nontoxic at low concentrations.<sup>88</sup>

In 2014, our group introduced stimuli-responsive end-caps to PGs to allow their triggered end-to-end depolymerization.<sup>89</sup> We polymerized ethyl glyoxylate (EtG) in CH<sub>2</sub>Cl<sub>2</sub> using catalytic

NEt<sub>3</sub> at -20 °C to afford **PEtG (Scheme 7a)**. Rigorous purification of the commercial EtG, through distillation over P<sub>2</sub>O<sub>5</sub>, was critical to depolymerize oligomers, and dehydrate the EtG hydrate. Based on size exclusion chromatography and end-group analysis using NMR spectroscopy, the polymerization is initiated by trace EtG hydrate. Thus, the molar mass of PGs is strongly dependent on the monomer purity. We have reported PEtGs with M<sub>n</sub> values between ~5–250 kg/mol and *D* of 1.4–2.1. Initially, 6-nitroveratryl carbonate (**NVOC**) was introduced as a stimuli-responsive end-cap, allowing depolymerization to be induced by UV light.<sup>89</sup> It was later expanded to other stimuli including reducing thiols (**DS**, **Azo**), H<sub>2</sub>O<sub>2</sub> (**AB**), acid (**Trit**, **MMT**, **DMT**), heat (**DA**), and multiple stimuli (light, reducing agents, and H<sub>2</sub>O<sub>2</sub>; **MS**) (**Scheme 7a**).<sup>90-92</sup>



**Scheme 7. (a)** Synthesis of PEtGs with different end-caps, its depolymerization back to monomer, and eventual monomer hydration and hydrolysis to afford GAH; **(b)** Synthesis of different glyoxylates from their fumaric or maleic acid esters.

In addition to **EtG**, other glyoxylate monomers were synthesized and polymerized. We prepared methyl glyoxylate (**MeG**), *n*-butyl glyoxylate (**BuG**), benzyl glyoxylate (**BzG**) and *L*-menthyl glyoxylate (**MenG**) from their corresponding maleic or fumaric diesters (**11**) by ozonolysis under reducing conditions (**Scheme 7b**).<sup>89, 93</sup> So far, a key criterion for obtaining pure monomer has been the ability to purify the glyoxylate by distillation over P<sub>2</sub>O<sub>5</sub>, at less than 165 °C, as the P<sub>2</sub>O<sub>5</sub> drying byproduct H<sub>3</sub>PO<sub>4</sub> contaminates the distillate at higher temperatures. Other drying agents such as CaH<sub>2</sub> resulted in slow cracking of oligomers and impure product.<sup>94</sup> In addition, the monomer precursors must be stable to ozonolysis, preventing the incorporation of double and triple bonds as pendant groups, as they would undesirably be cleaved by ozonolysis. We polymerized **MeG**, **BuG**, **BzG**, and **MenG**, and copolymerized them with **EtG**.<sup>89, 93</sup> The homopolymers had low M<sub>n</sub> (2.1–3.8 kg/mol), which can in some cases be attributed to steric hindrance (e.g., **BuG**, **MenG**). However, it has also been challenging to achieve purities as high as we achieved for EtG. With further optimization of the monomer distillation process, higher DP<sub>n</sub>s will likely be achieved. In contrast, copolymers of the different glyoxylates with EtG typically had relatively high DP<sub>n</sub>s (M<sub>n</sub> ranging from 30–40 kg/mol), suggesting that this approach mitigates issues of monomer purity and steric hindrance.

In addition to the NEt<sub>3</sub>-mediated polymerization method, anionic polymerization of glyoxylates has also been investigated. Moore and coworkers used *n*-BuLi as an initiator for EtG polymerization and end-capped the resulting polymer with phenyl isocyanate.<sup>95</sup> However, the fact that the resulting polymer had two end-caps, based on NMR spectroscopy, suggested that the

polymerization was not directly initiated from *n*-BuLi. Instead, EtG hydrate quickly quenched the *n*-BuLi, producing hydrate-based initiators that grew bidirectionally, resulting in two polymer termini that were later end-capped. To address this, we developed and reported a rigorous purification procedure for EtG and re-explored its anionic polymerization.<sup>94</sup> Initiation with *n*-BuLi at 20 °C, followed by cooling to -20 °C for 10 min, led to good dispersity values ( $D \sim 1.5$ ) and good control over  $DP_n$  up to  $\sim 200$  repeating units ( $M_n \sim 20$  kg/mol). Beyond this, the concentration of added initiator became so low that even trace hydrate initiators became significant and the  $DP_n$  deviated from the expected value. Up to a  $DP_n$  of 200, the end-group fidelity was greater than 90%, dropping to 71% at a targeted  $DP_n$  of 400. Different alkyllithium reagents and alkoxides were also effective initiators.

Moore and coworkers have also investigated the cationic polymerization of EtG using different initiators such as  $BF_3 \cdot OEt_2$ ,  $SnCl_4$ , and  $Ph_3CBF_4$ .<sup>95</sup> No end groups were found on cationically synthesized PEtG, suggesting a cyclic structure. Based on mass spectrometry results, Lewis acid initiators and high monomer concentrations led to backbiting of the growing PEtG chain on a pendant ester, leading to loss of an ethyl group. On the other hand, lower concentrations and carbocationic initiators led to backbiting on the backbone acetal. Both cyclic and lariat-shaped polymers were formed. Cationic copolymerization of EtG and *o*-PA was used to reduce the brittleness of PPA and increase its thermal stability.<sup>95</sup> The  $T_g$  and decomposition temperatures varied according to the ratio of monomers, with higher EtG leading to lower  $T_g$  and increased decomposition temperature.

PGs are attractive for biomedical applications as they eventually degrade to GAH, a metabolic intermediate. We prepared PEG-PEtG-PEG block copolymers by first introducing a linker end-cap containing both a photo-responsive moiety and a terminal alkyne (**Scheme 7a**,

**NVOC-link**), and then attaching the PEG blocks using copper-assisted azide-alkyne cycloaddition (CuAAC).<sup>89</sup> The resulting amphiphilic block copolymers were self-assembled to form micelles in aqueous solutions. Irradiation with UV light led to the depolymerization and disintegration of the micelles in less than 1 h. The approach was also extended to linker end-caps such as **DS** and **AB-link** (**Scheme 7a**), which are responsive to reducing thiols and H<sub>2</sub>O<sub>2</sub> respectively.<sup>96</sup> These stimuli are intrinsically present in the body and are associated with inflammation and cancer. Conjugation of PEG *via* disulfide exchange or CuAAC led to triblock copolymers that could also be self-assembled to form micelles. Treatment with the appropriate stimulus led to rapid depolymerization and micelle disintegration. The micelles were used to encapsulate Nile red, Dox, and curcumin. All payloads were rapidly released in the presence of low concentrations of stimuli, suggesting an amplification effect.

In the course of the work on PEG-PEtG-PEG micelles, we found that not all of the drugs we investigated could be encapsulated at high loadings into the PEtG micelle core. This was addressed by changing the pendant groups on the PG block.<sup>93</sup> By incorporating **BuG**, **MenG**, or chloral (non-glyoxylate aldehyde), we tuned the hydrophobicity of the micelle core and its compatibility with the drug celecoxib. Cytotoxicity studies were performed on the micelles in MDA-MB-231 human breast cancer cells. The different glyoxylate systems had different effects on cell metabolic activity and the degraded (triggered) micelles had different effects than the intact micelles. However, caution must be used in interpreting the results of these studies, as it is known that degradation products such as glyoxylate and ethanol can be metabolized in the liver but not in MDA-MB-231 cells.<sup>88</sup>

Using a thermally-triggerable PEG-PEtG-PEG triblock copolymer that was prepared using the **DA-link** end-cap (**Scheme 7a**), capable of undergoing a retro-Diels-Alder-elimination cascade,

we also investigated the indirect triggering of nanoassemblies in collaboration with the Sandre group.<sup>91</sup> A 63 kg/mol PEtG block was coupled to either 750 or 5000 g/mol PEG, leading to vesicle and micellar assemblies respectively (**Figure 10a,b**). Direct triggering of PEtG was achieved by heating the assemblies at 75 °C. For indirect triggering, we encapsulated iron oxide nanoparticles (IONPs) into the micelle cores (**Figure 10c**). Oscillating magnetic fields are known to induce localized heating around IONPs, an effect termed magnetic field hyperthermia (MFH).<sup>97</sup> MFH led to a rapid increase in particle diameter and decrease in DLS count rate for the IONP-loaded micelles, which was attributed to their depolymerization followed by aggregation and sedimentation of the released hydrophobic IONPs.

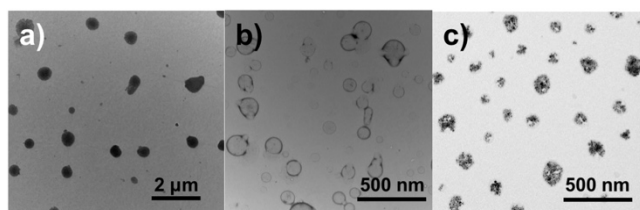


**Figure 10.** TEM images of assemblies formed from thermo-responsive PEG-PEtG-PEG triblock copolymers **(a)** micelles; **(b)** vesicles; **(c)** IONP-loaded micelles. Adapted with permission from reference <sup>91</sup>. Copyright 2017, Royal Society of Chemistry.

We also prepared PEtG-based particles for drug delivery applications by using an emulsion process.<sup>98</sup> We blended PEtG with PLA to achieve a two-stage release process, where a portion of loaded drug was released through an initial triggered depolymerization of PEtG, and a slower second-stage release occurred through the gradual degradation of PLA. Both **NVOC** and **DS** end-capped PEtG were used and gave particles with diameters of 130–150 nm. The particles were loaded with Nile red as a probe and with the drug celecoxib. In each case, the extent of release following triggering with the stimulus (UV light or DTT) increased with an increasing PEtG:PLA ratio, showing in principle that the extent of initial release could be tuned according to the particle



composition. However, in cytotoxicity studies with MDA-MB-231 cells we found that the sodium cholate surfactant was relatively toxic. Thus, less toxic surfactant should be used in future studies.

While the above work involved PG-based assemblies in solution, we also investigated the solid state depolymerization of PEtG. For example, **PEtG-NVOC (Scheme 7)** films were immersed in aqueous buffer solutions at pH 3 to 8.<sup>92</sup> For irradiated films, the degradation rate depended on the pH, with a rate minimum at pH 5, consistent with a hemiacetal fragmentation mechanism. The degradation time was also dependent on the film thickness. For instance, a 25  $\mu\text{m}$  thick film required 3 days for complete erosion and increasing the film thickness to 150  $\mu\text{m}$  increased the time to 10 days. Another determining factor was the temperature as much faster erosion was observed at 30 °C compared to that at 20 °C. We also found that the degradation rate was not dependent on the presence of water, and complete depolymerization was observed in the dry solid state.<sup>92</sup> In the absence of water, the monomer remains unhydrated. With a boiling point of 110 °C, EtG can readily evaporate from the surface. We used this feature to demonstrate single step micropatterning as well as a depolymerization-repolymerization sequence.

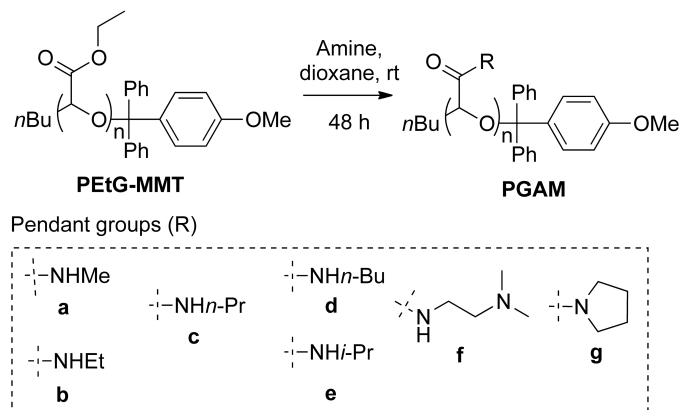
While **PEtG-NVOC** films are very stable in the absence of UV light, we observed that trityl end-capped PEtGs such as **PEtG-MMT** and **PEtG-DMT (Scheme 6a)** were surprisingly unstable in the solid state.<sup>99</sup> For example, films of **PEtG-DMT** were stable for more than 30 days at 6 °C, but completely degraded in less than 5 days at 30 °C. **PEtG-MMT** films were more stable, requiring more than 30 days for complete depolymerization at 30 °C. We attributed this behavior to an equilibrium between the capped and uncapped polymer, the position of which depends on the stability of the corresponding trityl cation. In the uncapped state, depolymerization occurs and is irreversible due to evaporation of monomer from the surface. To demonstrate the potential application of the system as a thermal history sensor, we incorporated Nile red and IR-780 dyes

into the films. Depolymerization led to aggregation of the dyes and changed the colour of the films. We envision that these materials can potentially be used for smart packaging applications.

PEtG is an amorphous polymer with low  $T_g$  of about  $-10\text{ }^\circ\text{C}$ . Therefore, it forms tacky and rubbery coatings at ambient temperatures. To improve its properties, we recently blended **PEtG-NVOC** with polyesters including polycaprolactone (PCL), poly(lactic acid) and poly(R-3-hydroxybutyrate).<sup>100</sup> We found that PEtG exhibited micro-scale phase separation with the polyesters, resulting in glassy or crystalline polyester domains. The mechanical properties of the blends were intermediate between those of the corresponding homopolymers, indicating that it was possible to tune the physical properties of the films through blending and to achieve non-tacky films. For example, while PCL had a Young's modulus of 490 MPa and tensile strength of 13 MPa, the 50:50 PCL:PEtG blend has values of 192 MPa and 5 MPa respectively. Mass loss studies and SEM images of the films showed that light-triggered degradation of the PEtG blocks was achieved, leaving a porous matrix of polyester that eroded more slowly. These coatings may be useful for the controlled release of drugs or fertilizers, as the payload may be released through the porous eroded film.

**Polyglyoxylamides (PGAMs).** We recently reported PGAMs as a new class of SIPs with the aim of removing the hydrolytically labile pendant esters of PGs and enabling further structure-property tuning.<sup>90</sup> The PGAMs were synthesized by the reaction of PEtG with different amines at ambient temperatures for 48 hours (**Scheme 8**). High ( $> 95\%$ ) conversions of the esters to amides were obtained with a variety of primary amines, and with the secondary amine pyrrolidine. Other secondary amines led to lower conversions, suggesting steric hindrance impeded the reaction. Another consideration is that the PEtG end-cap must be stable under the amidation conditions. For example, the carbonate-based end-caps were cleaved during the amidation, leading to

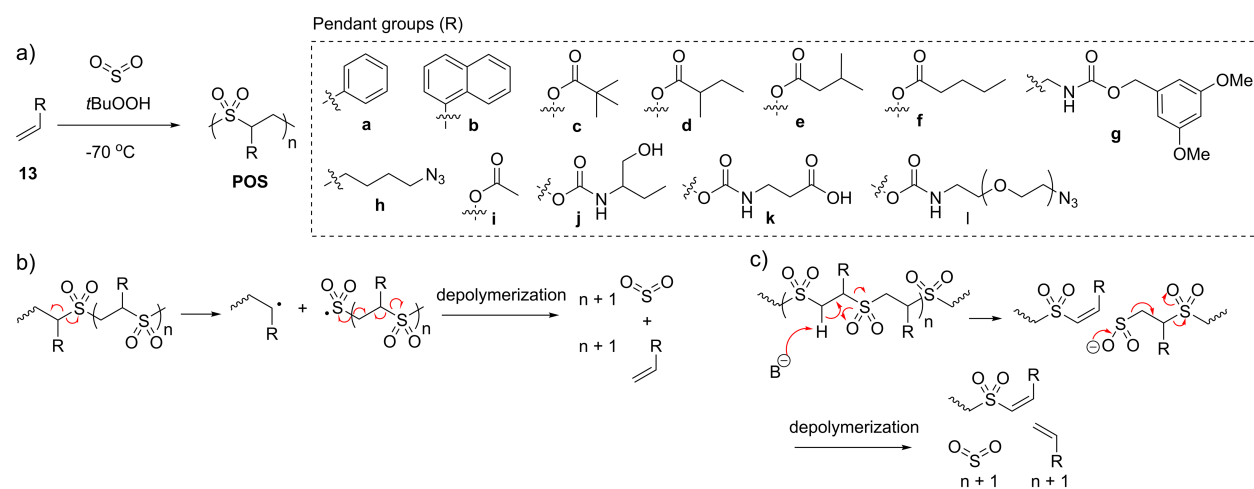
depolymerization, while trityl end-caps were stable. The depolymerization mechanism for PGAMs is the same as that of the polyglyoxylates, involving hemiacetal degradation, and produces the corresponding glyoxylamide hydrates as depolymerization products.



**Scheme 8.** Synthesis of PGAMs with different pendant groups starting from PETG with a MMT end-cap.

The PGAMs had very different properties than their corresponding esters. For example, PMeG and PETG have  $T_g$  values of 25 and  $-9$  °C respectively,<sup>89</sup> whereas poly(methyl glyoxylamide) (**PGAMa**) and poly(ethyl glyoxylamide) (**PGAMb**) have  $T_g$  values of 90 and 85 °C respectively.<sup>90</sup> These differences can be attributed to the abilities of the PGAMs to form hydrogen bonds. Some PGAMs (**PGAMa,f,g**) were soluble in water, opening opportunities for applications requiring water solubility. For example, in collaboration with Ree and Kelland we reported the study of PGAMs as kinetic hydrate inhibitors for the prevention of gas hydrate plugging in oil and gas lines.<sup>101</sup> Overall, there are many potential applications of PGAMs that remain unexplored. However, the limited availability of end-caps that are stable to the amidation reaction, yet undergo stimuli-selective cleavage is an ongoing challenge that must be addressed to fully exploit the PGAMs.

**Poly(olefin sulfone)s (POSSs).** POSSs are another class of low  $T_c$  polymers that has been exploited for their depolymerization behavior. They are composed of alternating  $\text{SO}_2$  and vinyl monomers (**13**), copolymerized *via* free-radical polymerization using initiators such as *tert*-butyl hydroperoxide (*t*BuOOH) in liquefied  $\text{SO}_2$  below  $-10\text{ }^\circ\text{C}$  (**Scheme 9a**).<sup>102-103</sup> Thus far, stimuli-responsive end-caps have not been incorporated into POSSs. Instead, the depolymerization has been initiated by random backbone cleavage at the relatively weak C-S bond, followed by entropically favoured release of gaseous  $\text{SO}_2$  and the corresponding vinyl monomer. The depolymerization can follow a free-radical (**Scheme 9b**)<sup>104</sup> or E2 elimination (**Scheme 9c**)<sup>105</sup> mechanism depending on the stimulus, conditions, and specific POS structure. In principle, the depolymerization products can be collected and repolymerized, although this has not yet been explicitly demonstrated. One advantage of the free-radical synthesis method of POSSs is its high functional group tolerance. A vast array of different vinyl monomers has been incorporated, some of which are depicted in **Scheme 9**. Depending on the vinyl monomer, POSSs generally have high  $T_g$ s, ranging from  $77\text{ }^\circ\text{C}$  for 1-hexadecene to  $177\text{--}200\text{ }^\circ\text{C}$  for styrene derivatives.<sup>102-103</sup>



**Scheme 9.** (a) Synthesis of POSSs, showing the incorporation of different vinyl monomers, and their depolymerization by (b) free-radical and (c) E2 mechanisms.

POSSs have been of significant interest for photolithography applications due to their depolymerization to volatile products in response to deep-UV and soft-X-ray irradiation. Early examples included **POSa** and **PO Sb** (**Scheme 9**), which were cleaved by electron beams and UV light.<sup>102-103</sup> Fréchet and coworkers investigated poly(*t*-butyl vinyl carbonate sulfone) (**POSc**), and found that while the polymer exhibited high lability to X-ray radiation and self-development capabilities, it did not have sufficient thermal stability to serve as a resist material.<sup>106</sup> Moore and coworkers recently showed that the degradation temperature could be tuned from 91–213 °C using different isomeric butyl carbonate side chains (**POSc-f**), with increased branching at the  $\beta$ -carbon to the carbonyl group leading to higher thermal stability.<sup>107</sup> To enhance the sensitivity of POSSs to UV light, a number of groups have also explored the incorporation of photobase generators (PBGs) as pendant groups (e.g., **PO Sg**) which can accelerate light-mediated backbone cleavage by the E2 mechanism.<sup>105</sup>

More recently, other applications of POSSs have been explored. For example, Lobe and Swager employed POSSs in smart composite materials.<sup>108</sup> A POSS with pendant azide moieties (**POSh**, **Scheme 9**) was functionalized with pyrene to enhance its compatibility with multiwalled carbon nanotubes (MWCNTs) and with a bismuth complex to enhance sensitivity towards ionizing radiation. Exposure of devices composed of the POSS and MWCNTs to gamma irradiation resulted in the depolymerization of the POSS, increasing connectivity between the MWCNTs, and providing a signal. It was proposed that the resulting sensors could be used for the detection and dosimetry of ionizing radiation in applications such as national security and nuclear research. Using the pendant azides on **POSh**, Lobe and Swager also prepared elastomeric composites *via* CuAAC-mediated conjugation to an alkyne-functionalized polydimethylsiloxane.<sup>109</sup> The mechanical properties of the composites were tuned based on the polymer ratios, lengths, and cross-linking

density. The composites were broken down by piperidine, and the process was visualized by the release of a dye molecule. Depolymerization of POS has also been exploited for the development of detachable adhesives. Sasaki and coworkers used a POS composed of volatile olefin and cross-linkable carboxylic acid moieties, with a PBG between two glass slides (**Figure 11**).<sup>110</sup> Curing with a carbodiimide resulted in strong adhesion of the slides. After irradiation and heating at 100 °C, the adhesive strength decreased by 50% after 5 min, and almost completely disappeared after 1 h.

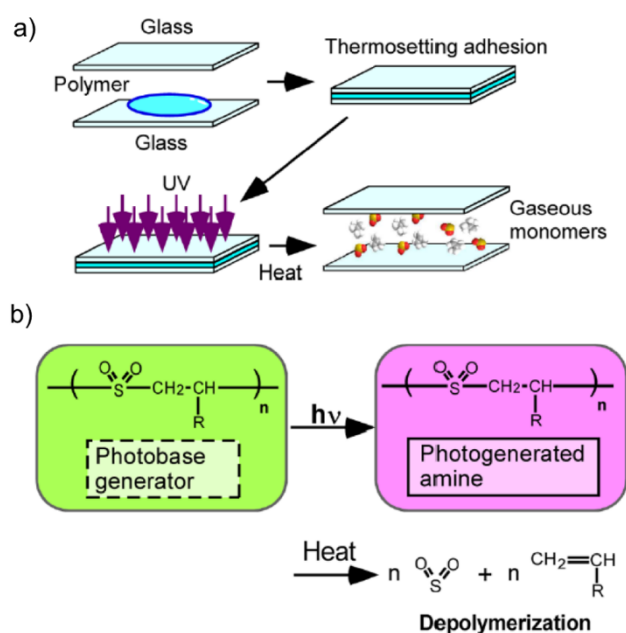


**Figure 11.** (a) A POS composed of a volatile olefin and a cross-linkable carboxylic acid-functionalized olefin was deposited between glass slides with a PBG and a cross-linker, and then thermally cured leading to adhesion of the slides. Irradiation with UV light, followed by heating to release volatile monomer detached the surfaces. (b) Schematic showing the conversion of PBG to amine base, then the resulting depolymerization and volatilization of the POS with heat. Adapted with permission from reference <sup>110</sup>. Copyright 2016, American Chemical Society.

Goodwin and coworkers explored the potential for POSs in drug delivery applications. They showed that poly(vinyl acetate sulfone) (**POSi**, **Scheme 9**) could be triggered to depolymerize by reactive oxygen species such as  $\text{Ca}(\text{OCl})_2$ ,  $\text{FeCl}_2/\text{H}_2\text{O}_2$ ,  $\text{KO}_2$ , and  $\text{NaOCl}$ , and by mechanical activation with ultrasound.<sup>111</sup> While the conditions were relatively harsh, the potential for POS to be cleaved by more biologically relevant stimuli was demonstrated. They also prepared a series of different poly(vinyl carbamate sulfone)s (e.g., **POSj-I**, **Scheme 9**).<sup>112</sup> Polymer **POSi** was then used for the preparation of dye-loaded nanoparticles *via* a nanoprecipitation process. The particles underwent degradation more rapidly at pH 7.0–7.4 than at pH 5.3, presumably due to the more rapid E2 elimination-based degradation at higher pH. Because of their increased susceptibility to degradation at neutral compared to mildly acidic pH, the particles were proposed for mucosal delivery, and the release of dyes in simulated mucosal fluid was demonstrated. While promising, further work will be needed to explore the stability of POSs in biological media as well as the toxicity of their depolymerization products.

## Perspective and outlook

In the growing quest for “smart” degradable materials, interest in SIPs has steadily increased over the past decade. Different backbones have been explored and applied to a vast array of different applications. Properties of some of the different backbones are summarized in Table 1. Each backbone has its own advantages and limitations in terms of synthetic access, physical and toxicological properties, as well as depolymerization kinetics in solution and the solid state. Thus, it is important to select an appropriate backbone for a given application.

**Table 1.** Summary of different SIP backbones.

Backbone	Monomer synthesis	Polymer synthesis	Depolymerization mechanism	Physical properties	Applications
PBC	1 step from commercial material	Sn(IV) catalysed step-growth polymerization	1,6-elimination-decarboxylation	Not reported	Sensors, drug delivery, activity linked labeling of enzymes
PBC with linkers	6 step (total) convergent synthesis	DMAP catalyzed step-growth polymerization	Cyclization-1,6-elimination-decarboxylation	Not reported	Drug delivery
PPA	Commercially available monomer; challenging syntheses of other monomers	Anionic (linear) or cationic (cyclic) chain addition polymerization	Hemiacetal fragmentation	Majority are high $T_g$ , brittle solids; tunable through copolymerization and use of additives	Lithography, transient electronics, smart composites, microscale pumps
PGs	Purify commercial monomer or synthesize in 2 steps	Proton transfer, anionic, or cationic chain addition polymerization	Hemiacetal fragmentation	Low $T_g$ for PEtG, variable for other PGs and for PGAMs, tunable through blending	Drug delivery smart coatings, thermal sensors
POS	Commercially available or custom-synthesized	Free radical chain addition polymerization	Free radical or E2 elimination	Highly dependent on vinyl monomer	Lithography, smart composites and adhesives, drug delivery
PBE	3 steps	Anionic chain addition polymerization	1,6-elimination	High $T_g$ and high thermal stability	Mixed plastics recycling, antibacterials

While new depolymerizable backbones have been continually introduced over the last decade, and older low  $T_c$  polymers have been endowed with new stimuli-responsive properties,



there are still a limited number of backbones. In our view, the introduction of new backbones is hindered by a few key challenges. In the area of irreversible SIPs, where depolymerization is generally based on cyclization of nucleophilic groups or elimination reactions involving electron-rich aromatics, careful monomer and polymer design are required so that the reactive groups are not revealed during polymerization so as to introduce competing self-immolative reactions. In the field of reversible SIPs,  $T_c$  values falling within a limited range of temperatures are required for successful backbone development. Generally, it is desirable that the  $T_c$  be at or below room temperature so that the polymer will spontaneously depolymerize upon triggering. In some applications, it may be acceptable to have a  $T_c$  somewhat above room temperature. However, at much elevated temperatures other undesirable reactions may occur. On the other hand,  $T_c$  defines the temperature below which depolymerization must be performed, and to obtain high conversion of monomer it should generally be performed well below  $T_c$ . Most irreversible SIPs have been synthesized at -78 to -10 °C. Below these temperatures, slow polymerization kinetics, low monomer and polymer solubility, and practical difficulties in performing the polymerization reaction become challenges. Thus, the  $T_c$  should ideally fall in the range of *ca.* -40 to 20 °C, and careful selection and/or modification of monomers is required in order to achieve this.

In terms of applications, it is important to consider where the key feature of depolymerization and amplification of the triggering signal can offer benefits beyond those of traditional degradable polymers. Even for well-established polymers such as poly(L-lactide), cost has been a barrier to their widespread use, as the prices of competing products such as polyethylene and poly(ethylene terephthalate) are much lower. It is likely the cost barriers would be even higher for SIPs. Therefore, it is unlikely at this stage that SIPs would be used in large scale commodity applications. Instead, they are more likely to find use in niche areas such as self-destructing

devices, lithography, sensors, or smart coatings which truly take advantage of their amplified responses to stimuli. Even for these applications, there are additional barriers aside from cost, such as requirements to change procedures and instrumentation in manufacturing processes, which hinder the introduction of new materials. In addition, in some cases it will be important to tune the physical properties of SIPs. For example, PPA is a brittle solid, while PEtG is a tacky rubbery material at room temperature. There have been some recent advancements in tuning these properties through the formation of copolymers, blends with other polymers and additives, and in the preparation of composites, but further efforts will be needed. Ultimately, the required properties will depend on their application.

SIPs have been of particular interest for biomedical applications, as the changes in conditions are often subtle *in vivo*, and the concentrations of biological stimuli are very low. The ability to achieve amplified responses to stimuli offers the potential for enhancing the release of drugs or other molecules at specific sites *in vivo*. So far, various classes of SIPs have been used in the preparation of micelles, vesicles, nanoparticles, and microcapsules. Cost will likely not be a major issue for the use of SIPs in biomedical applications due to the relatively high value of the payloads that they carry. However, further work will be needed to explore the toxicities of the polymers and their host responses *in vivo*. Even with this data, there is always significant hesitancy to adopt new polymers as translation can be achieved more quickly using polymers that are already approved for some applications. Therefore, it will be important to continue work in academic laboratories and to engage companies with a long-term vision for developing new products.

In conclusion, there have been many advancements in SIPs, particularly over the past decade. Nevertheless, tremendous opportunities still exist for the development of new SIPs with enhanced properties and depolymerization behavior and for their application in many different

areas, some of which certainly remain unexplored to date. The key for SIPs to enter the marketplace in commercial products will be to find applications where their unique depolymerization behavior can be exploited, while at the same time providing suitable properties that are compatible with their applications.

### **Acknowledgements**

We thank the Natural Sciences and Engineering Research Council of Canada (Stecie Award 507348-2017 and Strategic Project Grant 478981-2015 to ERG and Graduate Scholarship to REY) for funding.

### **References**

- (1) Haward, M. Plastic Pollution of the World's Seas and Oceans as a Contemporary Challenge in Ocean Governance. *Nat. Commun.* **2018**, *9*, 667.
- (2) Rochman, C. M. Microplastics Research—from Sink to Source. *Science* **2018**, *360*, 28–29.
- (3) Nicolas, J.; Mura, S.; Brambilla, D.; Mackiewicz, N.; Couvreur, P. Design, Functionalization Strategies and Biomedical Applications of Targeted Biodegradable/Biocompatible Polymer-Based Nanocarriers for Drug Delivery. *Chem. Soc. Rev.* **2013**, *42*, 1147–1235.
- (4) Langer, R.; Vacanti, J. Advances in Tissue Engineering. *J. Pediatr. Surg.* **2016**, *51*, 8–12.
- (5) Pushpamalar, J.; Veeramachineni, A. K.; Owh, C.; Loh, X. J. Biodegradable Polysaccharides for Controlled Drug Delivery. *ChemPlusChem* **2016**, *81*, 504–514.
- (6) Tyler, B.; Gullotti, D.; Mangraviti, A.; Utsuki, T.; Brem, H. Polylactic Acid (PLA) Controlled Delivery Carriers for Biomedical Applications. *Adv. Drug Delivery Rev.* **2016**, *107*, 163–175.

- (7) Pitt, G. G.; Gratzl, M. M.; Kimmel, G. L.; Surlles, J.; Sohindler, A. Aliphatic Polyesters II. The Degradation of Poly (DL-Lactide), Poly ( $\epsilon$ -Caprolactone), and Their Copolymers *in Vivo*. *Biomaterials* **1981**, *2*, 215–220.
- (8) Sagi, A.; Weinstain, R.; Karton, N.; Shabat, D. Self-Immolative Polymers. *J. Am. Chem. Soc.* **2008**, *130*, 5434–5435.
- (9) Phillips, S. T.; DiLauro, A. M. Continuous Head-to-Tail Depolymerization: An Emerging Concept for Imparting Amplified Responses to Stimuli-Responsive Materials. *ACS Macro Lett.* **2014**, *3*, 298–304.
- (10) DeWit, M. A.; Gillies, E. R. A Cascade Biodegradable Polymer Based on Alternating Cyclization and Elimination Reactions. *J. Am. Chem. Soc.* **2009**, *131*, 18327–18334.
- (11) Roth, M. E.; Green, O.; Gnaim, S.; Shabat, D. Dendritic, Oligomeric, and Polymeric Self-Immolative Molecular Amplification. *Chem. Rev.* **2016**, *116*, 1309–1352.
- (12) Wong, A. D.; DeWit, M. A.; Gillies, E. R. Amplified Release through the Stimulus Triggered Degradation of Self-Immolative Oligomers, Dendrimers, and Linear Polymers. *Adv. Drug Delivery Rev.* **2012**, *64*, 1031–1045.
- (13) Peterson, G. I.; Larsen, M. B.; Boydston, A. J. Controlled Depolymerization: Stimuli-Responsive Self-Immolative Polymers. *Macromolecules* **2012**, *45*, 7317–7328.
- (14) Amir, R. J.; Pessah, N.; Shamis, M.; Shabat, D. Self-Immolative Dendrimers. *Angew. Chem. Int. Ed.* **2003**, *42*, 4494–4499.
- (15) de Groot, F. M. H.; Albrecht, C.; Koekkoek, R.; Beusker, P. H.; Scheeren, H. W. "Cascade-Release Dendrimers" Liberate All End Groups Upon a Single Triggering Event in the Dendritic Core. *Angew. Chem., Int. Ed. Engl.* **2003**, *42*, 4490–4494.

- (16) Li, S.; Szalai, M. L.; Kevwitch, R. M.; McGrath, D. V. Dendrimer Disassembly by Benzyl Ether Depolymerization. *J. Am. Chem. Soc.* **2003**, *125*, 10516–10517.
- (17) Wu, Y.; Zhang, L.; Zhang, M.; Liu, Z.; Zhu, W.; Zhang, K. Bottlebrush Polymers with Self-Immolative Side Chains. *Polym. Chem.* **2018**, *9*, 1799–1806.
- (18) Carl, P. L.; Chakravarty, P. K.; Katzenellenbogen, J. A. A Novel Connector Linkage Applicable in Prodrug Design. *J. Med. Chem.* **1981**, *24*, 479–480.
- (19) Peterson, G. I.; Church, D. C.; Yakelis, N.; Boydston, A. 1,2-Oxazine Linker as a Thermal Trigger for Self-Immolative Polymers. *Polymer* **2014**, *55*, 5980–5985.
- (20) Wong, A. D.; Güngör, T. M.; Gillies, E. R. Multiresponsive Azobenzene End-Cap for Self-Immolative Polymers. *ACS Macro Lett.* **2014**, *3*, 1191–1195.
- (21) Weinstain, R.; Sagi, A.; Karton, N.; Shabat, D. Self-Immolative Comb-Polymers: Multiple-Release of Side-Reporters by a Single Stimulus Event. *Chem. - Eur. J.* **2008**, *14*, 6857–6861.
- (22) Robbins, J. S.; Schmid, K. M.; Phillips, S. T. Effects of Electronics, Aromaticity, and Solvent Polarity on the Rate of Azaquinone–Methide-Mediated Depolymerization of Aromatic Carbamate Oligomers. *J. Org. Chem.* **2013**, *78*, 3159–3169.
- (23) Gnaim, S.; Shabat, D. Self-Immolative Chemiluminescence Polymers: Innate Assimilation of Chemiexcitation in a Domino-Like Depolymerization. *J. Am. Chem. Soc.* **2017**, *139*, 10002–10008.
- (24) Scrimin, P.; Prins, L. J. Sensing through Signal Amplification. *Chem. Soc. Rev.* **2011**, *40*, 4488–4505.

- (25) Lewis, G. G.; Robbins, J. S.; Phillips, S. T. Phase-Switching Depolymerizable Poly(carbamate) Oligomers for Signal Amplification in Quantitative Time-Based Assays. *Macromolecules* **2013**, *46*, 5177–5183.
- (26) Lewis, G. G.; Robbins, J. S.; Phillips, S. T. A Prototype Point-of-Use Assay for Measuring Heavy Metal Contamination in Water Using Time as a Quantitative Readout. *Chem. Commun.* **2014**, *50*, 5352–5354.
- (27) Esser-Kahn, A. P.; Sottos, N. R.; White, S. R.; Moore, J. S. Programmable Microcapsules from Self-Immolative Polymers. *J. Am. Chem. Soc.* **2010**, *132*, 10266–10268.
- (28) Liu, G.; Wang, X.; Hu, J.; Zhang, G.; Liu, S. Self-Immolative Polymersomes for High-Efficiency Triggered Release and Programmed Enzymatic Reactions. *J. Am. Chem. Soc.* **2014**, *136*, 7492–7497.
- (29) Kuppusamy, P.; Li, H.; Ilangovan, G.; Cardounel, A. J.; Zweier, J. L.; Yamada, K.; Krishna, M. C.; Mitchell, J. B. Noninvasive Imaging of Tumor Redox Status and Its Modification by Tissue Glutathione Levels. *Cancer Res.* **2002**, *62*, 307–312.
- (30) Weinstain, R.; Baran, P. S.; Shabat, D. Activity-Linked Labeling of Enzymes by Self-Immolative Polymers. *Bioconjugate Chem.* **2009**, *20*, 1783–1791.
- (31) Saari, W. S.; Schwering, J. E.; Lyle, P. A.; Smith, S. J.; Engelhardt, E. L. Cyclization-Activated Prodrugs. Basic Carbamates of 4-Hydroxyanisole. *J. Med. Chem.* **1990**, *33*, 97–101.
- (32) Chen, E. K. Y.; McBride, R. A.; Gillies, E. R. Self-Immolative Polymers Containing Rapidly Cyclizing Spacers: Toward Rapid Depolymerization Rates. *Macromolecules* **2012**, *45*, 7364–7374.

- (33) Niskanen, J.; Wu, C.; Ostrowski, M.; Fuller, G. G.; Hietala, S.; Tenhu, H. Thermoresponsiveness of PDMAEMA. Electrostatic and Stereochemical Effects. *Macromolecules* **2013**, *46*, 2331–2340.
- (34) de Gracia Lux, C.; McFearin, C. L.; Joshi-Barr, S.; Sankaranarayanan, J.; Fomina, N.; Almutairi, A. Single UV or Near IR Triggering Event Leads to Polymer Degradation into Small Molecules. *ACS Macro Lett.* **2012**, *1*, 922–926.
- (35) Liu, G.; Zhang, G.; Hu, J.; Wang, X.; Zhu, M.; Liu, S. Hyperbranched Self-Immolative Polymers (HSIPS) for Programmed Payload Delivery and Ultrasensitive Detection. *J. Am. Chem. Soc.* **2015**, *137*, 11645–11655.
- (36) Penczek, S.; Load, G. Glossary of Terms Related to Kinetics, Thermodynamics, and Mechanisms of Polymerization. *Pure Appl. Chem.* **2008**, *80*, 2163–2193.
- (37) Uno, T.; Minari, M.; Kubo, M.; Itoh, T. Asymmetric Anionic Polymerization of 2,6-Dimethyl-7-Phenyl-1,4-Benzoquinone Methide. *J. Polym. Sci. A Polym. Chem.* **2004**, *42*, 4548–4555.
- (38) Olah, M. G.; Robbins, J. S.; Baker, M. S.; Phillips, S. T. End-Capped Poly(benzyl ethers): Acid and Base Stable Polymers That Depolymerize Rapidly from Head-to-Tail in Response to Specific Applied Signals. *Macromolecules* **2013**, *46*, 5924–5928.
- (39) Baker, M. S.; Kim, H.; Olah, M. G.; Lewis, G. G.; Phillips, S. T. Depolymerizable Poly(benzyl ether)-Based Materials for Selective Room Temperature Recycling. *Green Chem.* **2015**, *17*, 4541–4545.
- (40) Ergene, C.; Palermo, E. F. Self-Immolative Polymers with Potent and Selective Antibacterial Activity by Hydrophilic Side Chain Grafting. *J. Mater. Chem. B* **2018**, *6*, 7217–7229.

- (41) Ergene, C.; Palermo, E. F. Cationic Poly(benzyl ether)s as Self-Immolative Antimicrobial Polymers. *Biomacromolecules* **2017**, *18*, 3400–3409.
- (42) Xiao, Y.; Li, H.; Zhang, B.; Cheng, Z.; Li, Y.; Tan, X.; Zhang, K. Modulating the Depolymerization of Self-Immolative Brush Polymers with Poly(benzyl ether) Backbones. *Macromolecules* **2018**, *51*, 2899–2905.
- (43) Yeung, K.; Kim, H.; Mohapatra, H.; Phillips, S. T. Surface-Accessible Detection Units in Self-Immolative Polymers Enable Translation of Selective Molecular Detection Events into Amplified Responses in Macroscopic, Solid-State Plastics. *J. Am. Chem. Soc.* **2015**, *137*, 5324–5327.
- (44) Xiao, Y.; Li, Y.; Zhang, B.; Li, H.; Cheng, Z.; Shi, J.; Xiong, J.; Bai, Y.; Zhang, K. Functionalizable, Side Chain-Immolative Poly(benzyl ether)s. *ACS Macro Lett.* **2019**, *8*, 399–402.
- (45) Palermo, E. F.; Lienkamp, K.; Gillies, E. R.; Ragogna, P. J. Antibacterial Activity of Polymers: Discussions on the Nature of Amphiphilic Balance. *Angew. Chem.* **2019**, *131*, 3728–3731.
- (46) Riga, E. K.; Gillies, E.; Lienkamp, K. Self-Regenerating Antimicrobial Polymer Surfaces via Multilayer-Design—Sequential and Triggered Layer Shedding under Physiological Conditions. *Adv. Mater. Interfaces* **2019**, *6*, 1802049.
- (47) Wang, F.; Diesendruck, C. E. Polyphthalaldehyde: Synthesis, Derivatives, and Applications. *Macromol. Rapid Commun.* **2018**, *39*, 1700519.
- (48) Schwartz, J. M.; Engler, A.; Phillips, O.; Lee, J.; Kohl, P. A. Determination of Ceiling Temperature and Thermodynamic Properties of Low Ceiling Temperature Polyaldehydes. *J. Polym. Sci., Part A: Polym. Chem.* **2018**, *56*, 221–228.



- (49) Tagami, S.; Kagiya, T.; Aso, C. Polymerization of Aromatic Aldehydes. VII. Cyclopolymerization of *o*-Formylphenylacetaldehyde and Formation of a Cyclic Trimer. *Polym. J.* **1971**, *2*, 101–108.
- (50) Aso, C.; Tagami, S. Cyclopolymerization of *o*-Phthalaldehyde. *J. Polym. Sci., Part B: Polym. Phys.* **1967**, *5*, 217–220.
- (51) Ito, H.; Schwalm, R. Thermally Developable, Positive Resist Systems with High Sensitivity. *J. Electrochem. Soc.* **1989**, *136*, 241–245.
- (52) Kaitz, J. A.; Diesendruck, C. E.; Moore, J. S. End Group Characterization of Poly(phthalaldehyde): Surprising Discovery of a Reversible, Cationic Macrocyclization Mechanism. *J. Am. Chem. Soc.* **2013**, *135*, 12755–12761.
- (53) Kaitz, J. A.; Diesendruck, C. E.; Moore, J. S. Dynamic Covalent Macrocyclic Poly(phthalaldehyde)s: Scrambling Cyclic Homopolymer Mixtures Produces Multi-Block and Random Cyclic Copolymers. *Macromolecules* **2013**, *46*, 8121–8128.
- (54) Schwartz, J. M.; Phillips, O.; Engler, A.; Sutlief, A.; Lee, J.; Kohl, P. A. Stable, High-Molecular-Weight Poly(phthalaldehyde). *J. Polym. Sci., Part A: Polym. Chem.* **2017**, *55*, 1166–1172.
- (55) Engler, A.; Phillips, O.; Miller, R. C.; Tobin, C.; Kohl, P. A. Cationic Copolymerization of *o*-Phthalaldehyde and Functional Aliphatic Aldehydes. *Macromolecules* **2019**, *52*, 4020–4029.
- (56) Lopez Hernandez, H.; Takekuma, S. K.; Mejia, E. B.; Plantz, C. L.; Sottos, N. R.; Moore, J. S.; White, S. R. Processing-Dependent Mechanical Properties of Solvent Cast Cyclic Polyphthalaldehyde. *Polymer* **2019**, *162*, 29–34.
- (57) Jiang, J.; Warner, M.; Phillips, O.; Engler, A.; Kohl, P. A. Tunable Transient and Mechanical Properties of Photodegradable Poly(phthalaldehyde). *Polymer* **2019**, *176*, 206–212.

- (58) Ito, H.; Willson, C. G. Chemical Amplification in the Design of Dry Developing Resist Materials. *Polym. Eng. Sci.* **1983**, *23*, 1012–1018.
- (59) Ito, H.; England, W. P.; Ueda, M. Chemical Amplification Based on Acid-Catalyzed Depolymerization. *J. Photopolym. Sci. Tec.* **1990**, *3*, 219–233.
- (60) Ito, H.; Ueda, M.; Schwalm, R. Highly Sensitive Thermally Developable Positive Resist Systems. *J. Vac. Sci. Technol.* **1988**, *6*, 2259–2263.
- (61) Hernandez, H. L.; Kang, S.-K.; Lee, O. P.; Hwang, S.-W.; Kaitz, J. A.; Inci, B.; Park, C. W.; Chung, S.; Sottos, N. R.; Moore, J. S.; Rogers, J. A.; White, S. R. Triggered Transience of Metastable Poly(phthalaldehyde) for Transient Electronics. *Adv. Mater.* **2014**, *26*, 7637–7642.
- (62) Park, C. W.; Kang, S.-K.; Lopez Hernandez, H.; Kaitz, J. A.; Wie, D. S.; Shin, J.; Lee, O. P.; Sottos, N. R.; Moore, J. S.; Rogers, J. A.; White, S. R. Thermally Triggered Degradation of Transient Electronic Devices. *Adv. Mater.* **2015**, *27*, 3783–3788.
- (63) Lee, K. M.; Phillips, O.; Engler, A.; Kohl, P. A.; Rand, B. P. Phototriggered Depolymerization of Flexible Poly(phthalaldehyde) Substrates by Integrated Organic Light-Emitting Diodes. *ACS Appl. Mater. Interfaces* **2018**, *10*, 28062–28068.
- (64) Jiang, J.; Phillips, O.; Engler, A.; Vong, M. H.; Kohl, P. A. Photodegradable Transient Bilayered Poly(phthalaldehyde) with Improved Shelf Life. *Polym. Adv. Technol.* **2019**, *30*, 1198–1204.
- (65) Phillips, O.; Engler, A.; Schwartz, J. M.; Jiang, J.; Tobin, C.; Guta, Y. A.; Kohl, P. A. Sunlight Photodepolymerization of Transient Polymers. *J. Appl. Polym. Sci.* **2019**, *136*, 47141.
- (66) Diesendruck, C. E.; Peterson, G. I.; Kulik, H. J.; Kaitz, J. A.; Mar, B. D.; May, P. A.; White, S. R.; Martínez, T. J.; Boydston, A. J.; Moore, J. S. Mechanically Triggered Heterolytic Unzipping of a Low-Ceiling-Temperature Polymer. *Nat. Chem.* **2014**, *6*, 623.

- (67) Tang, S.; Tang, L.; Lu, X.; Liu, H.; Moore, J. S. Programmable Payload Release from Transient Polymer Microcapsules Triggered by a Specific Ion Coactivation Effect. *J. Am. Chem. Soc.* **2018**, *140*, 94–97.
- (68) Lloyd, E. M.; Lopez Hernandez, H.; Feinberg, A. M.; Yourdkhani, M.; Zen, E. K.; Mejia, E. B.; Sottos, N. R.; Moore, J. S.; White, S. R. Fully Recyclable Metastable Polymers and Composites. *Chem. Mater.* **2019**, *31*, 398–406.
- (69) Aso, C.; Tagami, S. Polymerization of Aromatic Aldehydes. III. The Cyclopolymerization of Phthalaldehyde and the Structure of the Polymer. *Macromolecules* **1969**, *2*, 414–419.
- (70) Seo, W.; Phillips, S. T. Patterned Plastics That Change Physical Structure in Response to Applied Chemical Signals. *J. Am. Chem. Soc.* **2010**, *132*, 9234–9235.
- (71) Coulembier, O.; Knoll, A.; Pires, D.; Gotsmann, B.; Duerig, U.; Frommer, J.; Miller, R. D.; Dubois, P.; Hedrick, J. L. Probe-Based Nanolithography: Self-Amplified Depolymerization Media for Dry Lithography. *Macromolecules* **2010**, *43*, 572–574.
- (72) Schwesinger, R.; Schlemper, H. Peralkylated Polyaminophosphazenes— Extremely Strong, Neutral Nitrogen Bases. *Angew. Chem., Int. Ed. Engl.* **1987**, *26*, 1167–1169.
- (73) DiLauro, A. M.; Robbins, J. S.; Phillips, S. T. Reproducible and Scalable Synthesis of End-Cap-Functionalized Depolymerizable Poly(phthalaldehydes). *Macromolecules* **2013**, *46*, 2963–2968.
- (74) DiLauro, A. M.; Abbaspourrad, A.; Weitz, D. A.; Phillips, S. T. Stimuli-Responsive Core–Shell Microcapsules with Tunable Rates of Release by Using a Depolymerizable Poly(phthalaldehyde) Membrane. *Macromolecules* **2013**, *46*, 3309–3313.

- (75) DiLauro, A. M.; Lewis, G. G.; Phillips, S. T. Self-Immolative Poly(4,5-dichlorophthalaldehyde) and Its Applications in Multi-Stimuli-Responsive Macroscopic Plastics. *Angew. Chem., Int. Ed. Engl.* **2015**, *127*, 6298–6303.
- (76) Kaitz, J. A.; Possanza, C. M.; Song, Y.; Diesendruck, C. E.; Spiering, A. J. H.; Meijer, E. W.; Moore, J. S. Depolymerizable, Adaptive Supramolecular Polymer Nanoparticles and Networks. *Polym. Chem.* **2014**, *5*, 3788–3794.
- (77) Kaitz, J. A.; Moore, J. S. Functional Phthalaldehyde Polymers by Copolymerization with Substituted Benzaldehydes. *Macromolecules* **2013**, *46*, 608–612.
- (78) de Marneffe, J.-F.; Chan, B. T.; Spieser, M.; Vereecke, G.; Naumov, S.; Vanhaeren, D.; Wolf, H.; Knoll, A. W. Conversion of a Patterned Organic Resist into a High Performance Inorganic Hard Mask for High Resolution Pattern Transfer. *ACS Nano* **2018**, *12*, 11152–11160.
- (79) Cheong, L. L.; Paul, P.; Holzner, F.; Despont, M.; Coady, D. J.; Hedrick, J. L.; Allen, R.; Knoll, A. W.; Duerig, U. Thermal Probe Maskless Lithography for 27.5 nm Half-Pitch Si Technology. *Nano Lett.* **2013**, *13*, 4485–4491.
- (80) Knoll, A. W.; Pires, D.; Coulembier, O.; Dubois, P.; Hedrick, J. L.; Frommer, J.; Duerig, U. Probe-Based 3-D Nanolithography Using Self-Amplified Depolymerization Polymers. *Adv. Mater.* **2010**, *22*, 3361–3365.
- (81) Skaug, M. J.; Schwemmer, C.; Fringes, S.; Rawlings, C. D.; Knoll, A. W. Nanofluidic Rocking Brownian Motors. *Science* **2018**, *359*, 1505–1508.
- (82) Zhang, H.; Yeung, K.; Robbins, J. S.; Pavlick, R. A.; Wu, M.; Liu, R.; Sen, A.; Phillips, S. T. Self-Powered Microscale Pumps Based on Analyte-Initiated Depolymerization Reactions. *Angew. Chem., Int. Ed. Engl.* **2012**, *51*, 2400–2404.

- (83) Burel, F.; Rossignol, L.; Pontvianne, P.; Hartman, J.; Couesnon, N.; Bunel, C. Synthesis and Characterization of Poly(ethyl glyoxylate) – a New Potentially Biodegradable Polymer. *e-Polym.* **2003**, *3*, 31.
- (84) Brachais, C. H.; Huguet, J.; Bunel, C. Synthesis, Characterization and Stabilization of Poly(methyl glyoxylate). *Polymer* **1997**, *38*, 4959–4964.
- (85) Crutchfield, M. M.; Papanu, V. D.; Warren, C. B. Polymeric Acetal Carboxylates. 1977, US Patent Application 4,144,226.
- (86) Belloncle, B.; Burel, F.; Oulyadi, H.; Bunel, C. Study of the *in vitro* Degradation of Poly(ethyl glyoxylate). *Polym. Degrad. Stab.* **2008**, *93*, 1151–1157.
- (87) Belloncle, B.; Bunel, C.; Menu-Bouaouiche, L.; Lesouhaitier, O.; Burel, F. Study of the Degradation of Poly(ethyl glyoxylate): Biodegradation, Toxicity and Ecotoxicity Assays. *J. Polym. Environ.* **2012**, *20*, 726–731.
- (88) Baker, P. R. S.; Cramer, S. D.; Kennedy, M.; Assimos, D. G.; Holmes, R. P. Glycolate and Glyoxylate Metabolism in HEPG2 Cells. *Am. J. Physiol.: Cell Physiol.* **2004**, *287*, C1359–C1365.
- (89) Fan, B.; Trant, J. F.; Wong, A. D.; Gillies, E. R. Polyglyoxylates: A Versatile Class of Triggerable Self-Immolative Polymers from Readily Accessible Monomers. *J. Am. Chem. Soc.* **2014**, *136*, 10116–10123.
- (90) Sirianni, Q. E. A.; Rabiee Kenaree, A.; Gillies, E. R. Polyglyoxylamides: Tuning Structure and Properties of Self-Immolative Polymers. *Macromolecules* **2019**, *52*, 262–270.
- (91) Fan, B.; Trant, J. F.; Hemery, G.; Sandre, O.; Gillies, E. R. Thermo-Responsive Self-Immolative Nanoassemblies: Direct and Indirect Triggering. *Chem. Commun.* **2017**, *53*, 12068–12071.

- (92) Fan, B.; Trant, J. F.; Yardley, R. E.; Pickering, A. J.; Lagugn -Labarthe, F.; Gillies, E. R. Photocontrolled Degradation of Stimuli-Responsive Poly(ethyl glyoxylate): Differentiating Features and Traceless Ambient Depolymerization. *Macromolecules* **2016**, *49*, 7196–7203.
- (93) Fan, B.; Yardley, R. E.; Trant, J. F.; Borecki, A.; Gillies, E. R. Tuning the Hydrophobic Cores of Self-Immolative Polyglyoxylate Assemblies. *Polym. Chem.* **2018**, *9*, 2601–2610.
- (94) Rabiee Kenaree, A.; Gillies, E. R. Controlled Polymerization of Ethyl Glyoxylate Using Alkylolithium and Alkoxide Initiators. *Macromolecules* **2018**, *51*, 5501–5510.
- (95) Kaitz, J. A.; Diesendruck, C. E.; Moore, J. S. Divergent Macrocyclization Mechanisms in the Cationic Initiated Polymerization of Ethyl Glyoxylate. *Macromolecules* **2014**, *47*, 3603–3607.
- (96) Fan, B.; Gillies, E. R. Poly(ethyl glyoxylate)-Poly(ethylene oxide) Nanoparticles: Stimuli-Responsive Drug Release *via* End-to-End Polyglyoxylate Depolymerization. *Mol. Pharm.* **2017**, *14*, 2548–2559.
- (97) P rigo, E. A.; Hemery, G.; Sandre, O.; Ortega, D.; Garaio, E.; Plazaola, F.; Teran, F. J. Fundamentals and Advances in Magnetic Hyperthermia. *Appl. Phys. Rev.* **2015**, *2*, 041302.
- (98) Gambles, M. T.; Fan, B.; Borecki, A.; Gillies, E. R. Hybrid Polyester Self-Immolative Polymer Nanoparticles for Controlled Drug Release. *ACS Omega* **2018**, *3*, 5002–5011.
- (99) Fan, B.; Salazar, R.; Gillies, E. R. Depolymerization of Trityl End-Capped Poly(ethyl glyoxylate): Potential Applications in Smart Packaging. *Macromol. Rapid Commun.* **2018**, *39*, 1800173.
- (100) Heuchan, S. M.; MacDonald, J. P.; Bauman, L. A.; Fan, B.; Henry, H. A. L.; Gillies, E. R. Photoinduced Degradation of Polymer Films Using Polyglyoxylate–Polyester Blends and Copolymers. *ACS Omega* **2018**, *3*, 18603–18612.

- (101) Ree, L. H. S.; Sirianni, Q. E. A.; Gillies, E. R.; Kelland, M. A. Systematic Study of Polyglyoxylamides as Powerful, High-Cloud-Point Kinetic Hydrate Inhibitors. *Energy Fuels* **2019**, *33*, 2067–2075.
- (102) Bowden, M. J.; Chandross, E. A. Poly(vinyl arene sulfones) as Novel Positive Photoresists. *J. Electrochem. Soc.* **1975**, *122*, 1370–1374.
- (103) Bowden, M. J.; Thompson, L. F. Poly(styrene sulfone)—a Sensitive Ion-Millable Positive Electron Beam Resist. *J. Electrochem. Soc.* **1974**, *121*, 1620–1623.
- (104) Brown, J. R.; O'Donnell, J. H.  $\gamma$  Radiolysis of Poly(butene-1 sulfone) and Poly(hexene-1 sulfone). *Macromolecules* **1972**, *5*, 109–114.
- (105) Sasaki, T.; Van Le, K.; Naka, Y., Alkenes. In *Alkenes*, Davarnejad, R. S., Baharak, Ed. InTechOpen: Online, 2017, pp 121–144.
- (106) Jiang, Y.; Frechet, J. M. J. Design and Synthesis of Thermally Labile Polymers for Microelectronics: Poly(vinyl tert-Butyl carbonate sulfone). *Macromolecules* **1991**, *24*, 3528–3532.
- (107) Lee, O. P.; Lopez Hernandez, H.; Moore, J. S. Tunable Thermal Degradation of Poly(vinyl butyl carbonate sulfone)s via Side-Chain Branching. *ACS Macro Lett.* **2015**, *4*, 665–668.
- (108) Lobez, J. M.; Swager, T. M. Radiation Detection: Resistivity Responses in Functional Poly(olefin sulfone)/Carbon Nanotube Composites. *Angew. Chem., Int. Ed. Engl.* **2010**, *49*, 95–98.
- (109) Lobez, J. M.; Swager, T. M. Disassembly of Elastomers: Poly(olefin sulfone)–Silicones with Switchable Mechanical Properties. *Macromolecules* **2010**, *43*, 10422–10426.
- (110) Sasaki, T.; Hashimoto, S.; Nogami, N.; Sugiyama, Y.; Mori, M.; Naka, Y.; Le, K. V. Dismantlable Thermosetting Adhesives Composed of a Cross-Linkable Poly(olefin sulfone) with a Photobase Generator. *ACS Appl. Mater. Interfaces* **2016**, *8*, 5580–5585.

- (111) Kumar, K.; Goodwin, A. P. Alternating Sulfone Copolymers Depolymerize in Response to Both Chemical and Mechanical Stimuli. *ACS Macro Lett.* **2015**, *4*, 907–911.
- (112) Kumar, K.; Castaño, E. J.; Weidner, A. R.; Yildirim, A.; Goodwin, A. P. Depolymerizable Poly(*O*-vinyl carbamate-*alt*-sulfones) as Customizable Macromolecular Scaffolds for Mucosal Drug Delivery. *ACS Macro Lett.* **2016**, *5*, 636–640.



## Biographies



Elizabeth Gillies was born and raised in Ontario, Canada and obtained her B.Sc. degree in Chemistry from Queen's University (Canada) in 2000. She then moved to the University of California, Berkeley where she worked with Jean Fréchet on polymer and dendrimer-based drug delivery systems. After completing her Ph.D. degree in 2004, she moved to the European Institute of Chemistry and Biology in France, working with Ivan Huc on helical foldamers. She joined the University of Western Ontario in 2006 and is currently a Professor in the Department of Chemistry and Department of Chemical and Biochemical Engineering. Her research group works on the development of self-immolative and other stimuli-responsive and biodegradable polymers, phosphorus-containing polymers, and polymer assemblies, as well as their applications in drug delivery, tissue engineering, functional coatings, and other areas. Dr. Gillies currently directs the Centre for Advanced Materials and Biomaterials Research at Western and has been recognized with a Canada Research Chair (2006-2016), Early Researcher Award (2008), and an NSERC E.W.R. Steacie Memorial Fellowship (2017).



Amir Rabiee Kenaree was born and grew up in Babol, a northern city in Iran, before he moved to Tehran where he obtained his B.Sc. degree in Chemistry in 2007 at the University of Tehran. There, he continued his education by joining the Prof. Caro Lucas' lab where he worked on the applications of artificial intelligence for simulating and modeling industrial processes to complete his M.Sc. degree in Chemical Engineering in 2010. After that, he worked as the CEO of an edible-oil manufacturing company, until he moved to the University of Western Ontario where he started his Ph.D. project under the supervision of Prof. Joe Gilroy in 2013. There he worked on the synthesis of metal-containing phosphines and their use in coordination, polymer, and materials science to complete his Ph.D. degree in 2016. He then joined the Gillies lab in 2017 and his research is focused on anionic polymerization methods in addition to developing new self-immolative materials based on new monomers, architectures, end-capping strategies, and building blocks.



Rebecca Yardley received her B.Sc. degree in Chemistry from Wilfrid Laurier University in Waterloo, ON, Canada, where she researched discotic liquid crystals under Prof. Kenneth Maly. She is currently a Ph.D. student in Polymer Chemistry at the University of Western Ontario under the direction of Prof. Elizabeth Gillies and has held an NSERC – Canada Graduate Scholarship. Her current research focuses on the development of novel glyoxylate monomers for use in self-immolative polymer systems.